Control design of a short-stroke workpiece actuator for error motion compensation

Pablo Carbonell Romero

Preface

Contents

Abstract

The prototype of a five axis ELID grinding machine is being developed at KU Leuven. The scope of this machine is the production of lenses with nanometer accuracy. For obtaining this level of precision a robust controller has to be designed to minimize the disturbances of the process. In previous theses a VCA (voice coil actuator) was studied an implemented. The aim of this project is to design a controller that uses the VCA to reject the disturbances created by the grinding forces as well as other disturbances.

The transfer function of the system has to be identified through excitation of the machine. Once the transfer function is obtained, the controller needs to be implemented. The first controller designed is a PID controller. A state space based controller has also been designed, but due to a problem with time delay it has not been implemented into the setup. While developing the controller, two problems have been encountered: time delay and bandwidth limiting resonance peaks. To solve time delay, a control structure called Smith predictor has been implemented into the machine. To compensate the bandwitdth limiting peaks, Notch filters have been designed and introduced into the control scheme.

With the controllers that have been designed, the last step is to see how the grinding machine performs under the effect of the disturbance produced by the rotary table. The table rotates at a speed of 12rpm. By adding the notch filters and the Smith predictor, an error of 56nm rms is obtained under a frequency of 260Hz.

List of Figures and Tables

List of Figures

List of Tables

List of Abbreviations and Symbols

Abbreviations

ELID	ELectrolytic In process Dressing
FF	FeedForward
FRF	Frequency Response Function
FVCA	Force of the voice coil actuator
ML	Maximum Likelihood
MIMO	Multiple Input Multiple Output
NLLM	Non Linear Least Squares
PID	Proportional Integral and Derivative
PM	Phase Margin
RLA	Rotatory Linear Actuator
RMS	Root mean square
SISO	Single-input single-output
VCA	Voice coil actuator
WMF	Workpiece metrology frame

Symbols

c	Damping coefficient
w	Frequency
k	Stiffness
L	Length
I	Inertia Moment
E	Elastic Modulus
m	Mass
π	The number pi
τ	Time delay
ϕ	Phase

Chapter 1

Introduction

1.1   Overall Goal

Free-form lenses have been slowly introduced in the industry. A review about the state of art of free-form lenses can be seen in [8]. In this article is also mentioned that nano-meter precision is needed to perform correct surfaces. The solution that the KU Leuven has developed in order to produce high quality and precision free-form lenses is the nano-grinding machine. There are a lot of free-form lenses applications, for example, applications in the scope of illumination like [14]. There are also another examples in the field of lenses for telescopes mentioned in [13]. The initial design of the grinding machine can be seen in the doctoral thesis of D. Hemschoote [9]. This machine, called the five-axis ELID grinding machine will be able to produce pieces with nanometer-precision tolerances for different applications and materials once finished.

1.2   Design of the Nano Grind

The main design of the machine has been developed in [9]. Nevertheless, some parts of the machine have been modified in posterior master theses. Those changes have to be taken into account while designing the controller.

The size of the machine designed is around $2m \times 2m \times 2m$. In the figure the different parts of the Nano Grind 1.1 can be seen. The baseframe allows the main frames to operate in their position. Also the yoke that is designed to move the orientation of the tool respect to the piece can be seen in the picture. The x-slide and the y-slide are already designed and constructed and allows the workpiece to move in both directions.
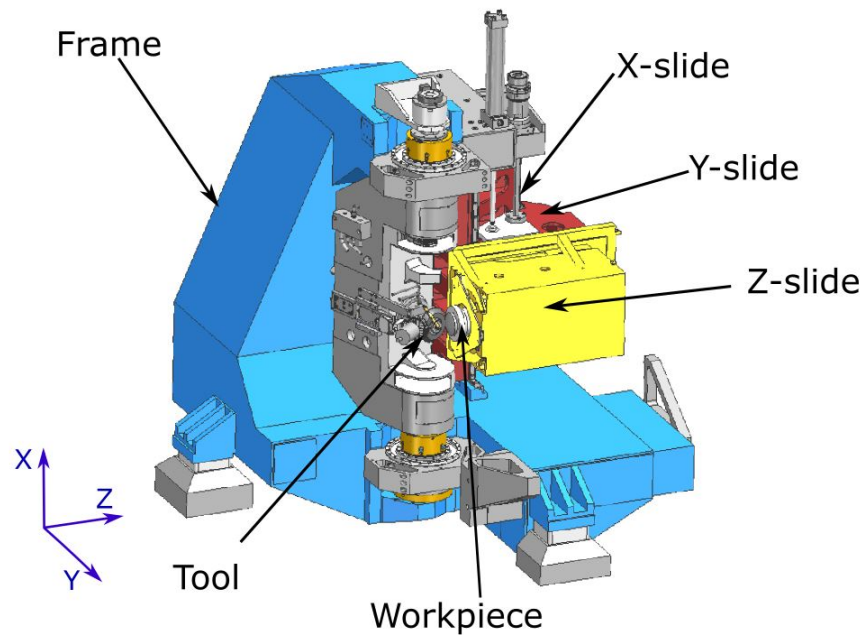
Figure 1.1: Nano Grind design

The part of the machine that is going to be treated corresponds to the z-frame that can be seen in the assembly of the whole machine. The parts of the machine that are already constructed can be seen in the figure 1.2. The first construction of the machine can be seen in [16]. It has also been enhanced with the WMF (Workpiece metrology frame) designed and constructed in [10]. This WMF is the measurement system that is capable of measuring the relative position between the tool and the workpiece. The shaft can move accurately without the use of expensive hydrostatic bearings thanks to the measurement information obtained by means of the sensors located in the machine.

By not using hydrostatic bearings, ball bearings have been used. This bearings are cheaper, however, they create high frequency errors motions. This errors can be measured but they cannot be compensated since the bandwidth of the slides is too low.
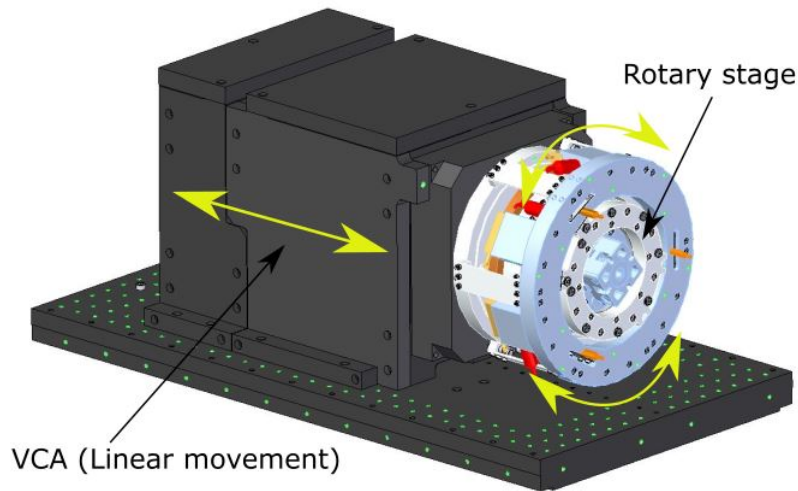
Figure 1.2: Z-slide in its current state.

As the RLA (Rotatory Linear Actuator) needs to be assembled, the z-slide has been constructed on top of a table. The axis in which is being modified is different to the one from which is going to operate at the end. The main function of the RLA built into the z-slide is to locate the piece into the position needed in order to reduce the error produced by another processes or disturbances from the grinding machine.

In the figure 1.2 the two actuator can be seen. The first one is the VCA (Voice Coil Actuator). The VCA is the one that produces the linear movement of the shaft of the machine. In following chapters the VCA will be better explained. The other actuator implemented in the machine is the rotary stage, and it is the one that produces the circular movement to orient the piece into the position desired.

1.3 Task Description

Based on the design of the machine that has been constructed, a controller for the linear stage mentioned above is going to be implemented. The controller has to be prepared to deal with different situations that can decrease the precision of the machined pieces.

1.3.1 Specifications

Because of the high frequency error motions, a faster actuator needs to be designed. This actuator needs to achieve certain specifications to compensate the errors. Some situations are going to be validated in the machine to prove the performance of the controller. The specifications for the three cases are the same in all situations. The following needs to be achieved: limiting the tracking error to 30nm (Root mean square) in the bandwidth between 0-10 Hz and 4 nm rms between 10-1000Hz. The

specifications mentioned are all measured with a volume at 100mm diameter and 30mm height above the workpiece pallet.

Positioning, effect of rotary table

Since the effect of the rotary table can modify the position of the workpiece, the z-displacement during rotation of the C-axis has to be controlled.

Positioning, effect of linear stage

Also the Z-displacement error during the translation of a virtual z-axis needs to be compensated.

Effect of process forces

The last step is the control of the z-displacement error over during grinding forces. For this purpose, recording forces of a real process is going to be used in order to reproduce grinding forces.

To achieve this values, some problems need to be solved. The main two problems are a phase lag produced by the data acquisition system and the error produced by the bearings at high frequencies. Both causes and solutions about those problems will be developed in the next chapters.

The controllers that have been selected for the system are, first, a traditional PID controller, then, a state space controller.

1.4 Outline of the thesis

Chapter 2 consists of a study about the different control methods that can be applied in order to achieve the best possible results. It also reviews the main problems that the thesis will face.

Chapter 3 analyses the physical model in which the machine can be simplified into. This model will take as account the WMF designed in previous thesis. The values of the sensors there implemented will be needed to control the system.

Chapter 4 determines the mathematical model in which the system can be represented as a result of several experiments that have been done in the machine. The model will help to have a clear idea about the control needed to design.

Chapter 5 designs and evaluates the behaviour of a PID controller implemented in the system. The results of the PID controller will be analysed in order to know if the control specifications are sufficient.

Chapter 6 evaluates the control of the system in optimal control. Some other aspects that can be done in optimal control such as modal filter of Smith Predictor will be explained and designed.

Chapter 7 shows how the different controllers are going to be implemented into the machine in order to be sure that the specifications mentioned above will be achieved.

Chapter 8 contains a general conclusion of the thesis here explained and also a guideline of how the future work should head to.

Chapter 2

Literature review

The goal of this thesis is the proper control over the Voice Coil Actuator under the effects of disturbances caused within or outside the grinding process. Some control methods have been applied in previous theses. In this thesis, another different methods of control are studied. The control of the VCA has to be really accurate since nano-precision tolerances have to be achieved. For this reason, a review over different schemes on control in high precision engineering is performed. Also, some of the problems mentioned in the introduction such as the time delay and the effect that high frequencies might have into high-speed control are treated.

2.1 Controller Scheme

2.1.1 PID Controller

The design and implementation of a PID controller is mentioned in this section. PID controller is the most famous and widely used controller in industry. This is due to its easy implementation and the low complexity when parametrized. PID controller is also the most studied controller in literature, since it can be applied to a high number or different processes.

In this thesis, PID controller is one of the control techniques applied to the process. The basis of this type of controller is a mathematic function that can be described as follows according to [5]:

$$u(t) = K_p e(t) + K_i \int_0^t e(\tau)d\tau + K_d \frac{de(t)}{dt} \tag{2.1}$$

Being K_p, K_i and K_d the Proportional, Integral and Derivative gains. e is the error signal, coming from $e = y - r$ where y is the output signal and r is the reference. The basic scheme of a PID controller corresponds to figure 2.1.
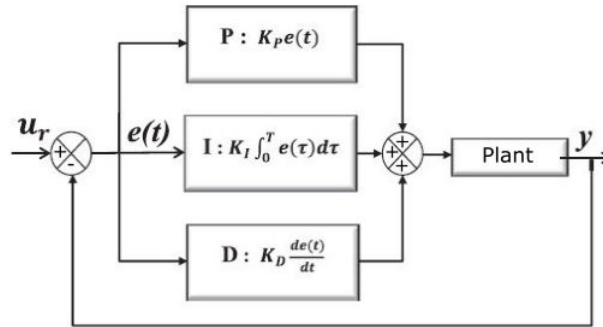
Figure 2.1: PID Scheme.

Also, the effect of the PID gains related with the behaviour of the response can be seen in figure 2.2 obtained from [1].

Closed-Loop Response	Rise Time	Overshoot	Settling Time	Steady-State Error	Stability
Increasing K_P	Decrease	Increase	Small Increase	Decrease	Degrade
Increasing K_I	Small Decrease	Increase	Increase	Large Decrease	Degrade
Increasing K_D	Small Decrease	Decrease	Decrease	Minor Change	Improve

Figure 2.2: Effect of the PID gains into the step response.

The different methodologies to tune the PID controllers are as wide as its range of application. There are a lot of different ways to select the parameters according to different criteria.

Time Response

Time domain methods use specifications such as settling time, overshoot and steady state error in order to tune the PID. For this reason, a study about the step response system needs to be performed to evaluate the parameters required. According to [12] frequency methods often makes use of correlations between frequency and time domain by using the second order poles, but this might not be always correct. Once the measurements about the step response are done, the parameters or the PID are chosen according to the new system specifications.

Frequency Response

A different methodology of chosing the parameters of the PID controller is to evaluate the frequency reponse. Graphic tools such as Bode plot or Nyquist plot are used as the representation of the system. Then, the parameters are chosen in order to match the requirements of the close loop response function. Both phase margin and gain margin are determinant to evaluate the performance of the controller. The advantage of those kind of methods is that they do not require the model of the plant of the model, just with the frequency response is enough. In this case, the information that is obtained from the system is the frequency response, so this kind of methods are the most suitable for the system treated in this thesis.

Ziegler−Nichols

Another method studied is the Ziegler−Nichols method. This heuristic method consists of looking into the step response in order to tune the parameters K_p, K_i and K_d. It is tuned in a way in which both derivative and integral gains are set to 0. Then, the K_p is increased until the system has stable oscillations. This gain is K_r and the period of the oscillations is T_r,then and the rest of the parameters can be chosen. The table 2.3 from [18] is based on a large number of experiments.

compensator	K/K_r	T_i/T_r	T_d/T_r
P	0.5		
PI	0.45	0.85	
PID	0.6	0.5	0.125

Figure 2.3: Table of the Ziegler-Nichols method

As mentioned in [3], the drawbacks of Ziegler-Nichols method is that they give the system poor robustness, and also it uses not enough process information. Since it gives poor robustness, this method is not used.

In addition, there are several other different ways of tuning a PID such as root-locus or another heuristic methods, but the ones above described were the ones taken into account.

2.1.2 State Space Controller

Space State scheme makes used of a system of matrices to modelize the physical system. This system has the appearance of formula 2.2:

$$\begin{cases} \dot{x} = Ax + Bu \\ y = Cx + Du \end{cases} \qquad (2.2)$$

9

The advantages of this control is that all the poles can be correctly placed and not just the dominant ones. Also it can handle way better MIMO (Multiple Inputs Multiple Outputs) systems. On the other hand, this tool does not provide a visual design as in frequency domain techniques in order to achieve the solution. The strategy of the control used in this technique will be shown in the chapter 4. The reason to use this kind of method is that it can be easily computed by software and provide a robust signal if the identification is properly done.

Since the system is just one degree of freedom but it requires a higher number of states, an estimator is required to estimate those unmeasured states. A short review of the estimators available is performed.

State Estimator

The state estimator is designed when the states are not directly measurable. The aim is to have the value of the states in order to compute the control law with them. It is calculated placing faster poles than the control matrix. The advantages of this estimator is the ease of both calculation and implementation but it does not take into account the noise that can appear in the system. Since the system studied is not really noisy, this estimator would suffice.

LQE

The LQE (Linear Quadratic Estimator) is a estimator for linear systems that takes into account the noise in within the system to perform the prediction. Both measurement and process noise are used to design the estimator. The advantage of this estimator is that according to [19] just one of the noise matrices is needed. The disadvantage is that is more complicated to implement than the state estimator and as mentioned, the system studied is not noisy, so this estimator is not used in this thesis.

Kalman Filter

The Kalman Filter is one of the most famous and widely used estimators. As the LQE, it takes both the measurement noise and the process noise. The Kalman Filter applies an algorithm in which in every step calculates the estimated states using the noise covariances. The problem with this estimator is that it is more complex to implement that the state estimator, so it has not to be taken into account while applying it into the State Space controller design. There is still some more ways and schemes of control that have not been mentioned. In past theses such as [11] H_∞ has been applied, because of that, another methods are explored.

2.2   Delay compensation

One of the main problems that appears in the system is time delay. This time delay can be seen by means of a phase lag in the frequency response once the system has

been identified. Time delay is a problem that appears in a huge number of different systems, such as chemical or thermal processes. Because of that some solutions have been studied and applied along the last century to neglect this time delay in the response of the system. Some of the methods to eliminate the effect of this delay are shown.

2.2.1 Smith Predictor

The Smith Predictor is one of the most known methods for time delayed systems. The working principle is to implement the plant of the system in a close loop but without the delay in order to neglect it from the system. According to [17] the performance of the Smith predictor can be around 30% better than with the use of just the PID controller. The drawback of this method is that it can have instabilities if a mismatch between the predicted plant and the real behaviour occurs but, in the case studied in this thesis, those mismatches are assume to not exist. This is because the system is assumed to be robust and not time variant over the working time. Smith Predictor has been historically used in long time delays but, in this case it would be used in a system with a short time delay in order to check if it also works in this kind of situations.

2.2.2 Direct Synthesis

In direct synthesis the design of the controller is based on the desired closed-loop transfer function. The controller then is computed analytically for the closed-loop set-point response to match the required response. As indicated in [17] the delay can be modelized into a high order polynomial function. Since direct synthesis methods are quite different from PID controllers it is not used in the thesis as a time delay compensation.

2.3 High frequency peaks control

The other problem that this thesis has to face is, as shown in next chapters, some frequency peaks that appear in the high frequency spectrum. This problem can affect to the bandwidth of the designed controller, so trying to neglect this peaks is studied. To solve this problem, some methods have been studied.

2.3.1 Notch Filters

The first studied method is the use of notch filters. This filters reduce the gain of a certain frequency and they can be used in resonance peaks in order to reduce their gain value. The transfer function of a notch filter is shown in figure 2.4.
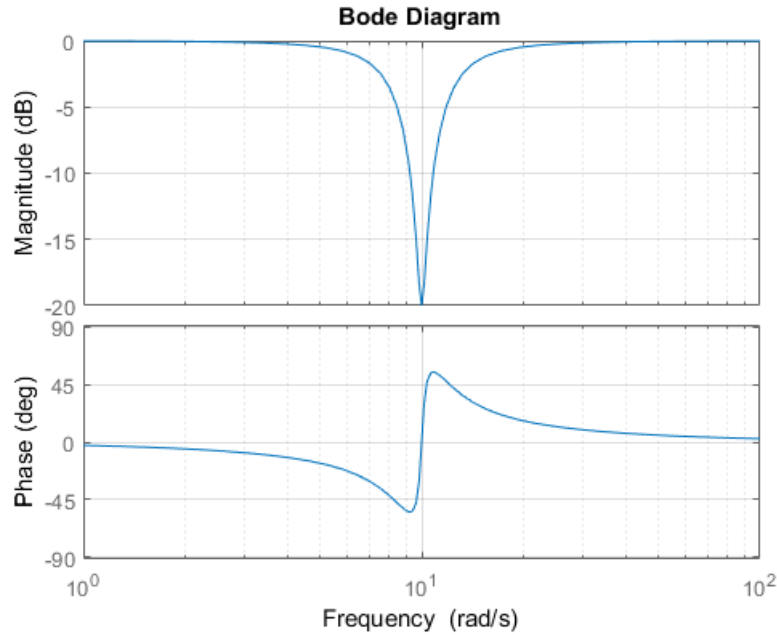
Figure 2.4: Transfer function of a notch filter

In [15] the effect of the notch filters has been mentioned for a nano-precision posi-
tioning. According to the paper, the disadvantage is that they introduce a lag in
the system and the phase margin tends to be smaller which can make the system
unstable. Since a lag compensation is studied, the effect of the notch filters are still
tested in the system as a solution to reduce the effect of the high frequency peaks.

2.3.2   Mode Decoupling

In [2] a different method to deal with bandwidth limiting resonance peaks for MIMO
systems is explained. This method offers a different solution than applying notch
filters, in order to not introduce the phase lag in the system. On this paper two
different solutions are offered. In the first solution, 2 sets of measurements have
been developed. The 2 sets of sensors are placed in a way that they cannot see the
mode that is tried to be filtered. Then, the frequency response is built by adding
a notch filter and an anti-notch filter in the frequency when the non-desired mode
is, and then, add them up. In the second solution, an extra sensor is added. When
measuring the flexible mode that corresponds to the non-desired mode, it can be
neglected from the measurement matrix by just setting the value to 0. Since the
measurement frame was already built, this solution has not been taken into account.

2.4   Conclusion

In this chapter, some of the main strategies of control have been reviewed. As a control representation, both PID controller and state space have been selected to proceed in order to design the controller. Regarding delay compensation, the Smith predictor has been taken into account in order to prevent the system from the effects of the delay. Finally, the introduction of the notch filter in the system has been selected in order to deal with the high frequency peaks that can make the control under-perform.

Chapter 3

Physical Modeling

In this chapter, an explanation about the system that is being controlled and the physical behaviour that is taken into account in developed. First an explanation about the z-slide that needs to be controlled is given. Secondly, a mass-spring-damper model is implemented using the appropriate physical parameters. The last part is an analysis about the model obtained.

3.1   The z-slide

The z-slide was mentioned in the introduction and now a better explanation is given. The z-slide has been first designed in [9] but the metrology frame has been modified and implemented by [10]. The main function of the RLA built into the z-slide is to locate the piece into the position needed in order to reduce the error produced by another processes or disturbances from the grinding machine.

In order to understand how to achieve the control of the machine itself, the different elements need to be studied. The overview of the RLA can be seen in 3.2. Since the elements in the black box cannot be seen, the upper cover has been removed. The inside can be seen in figure 3.1. To simplify, the parts have been presented in figure 3.3.

The different parts that are:

- Z-frame: Is the black box that supports the whole structure of the RLA. It is attached to the Y-slide.

- Countermass: It filters the forces from the VCA going to the frame of the z-slide.

- VCA: It is the actuator constituted by a coil and a magnet that allows the shaft to be displaced in any position between the range of the actuator.

- Shaft: It is the piece that follows the movement created by both the rotatory and the linear stage. It is hollow in the middle.

- Flexure: They are disks that create the union between the z-frame and the countermass, as well as with another rotatory elements. The flexure of the rotatory table union moves the shaft relatively to the rotation table and the flexure of the countermass moves the countermass relative to the frame.
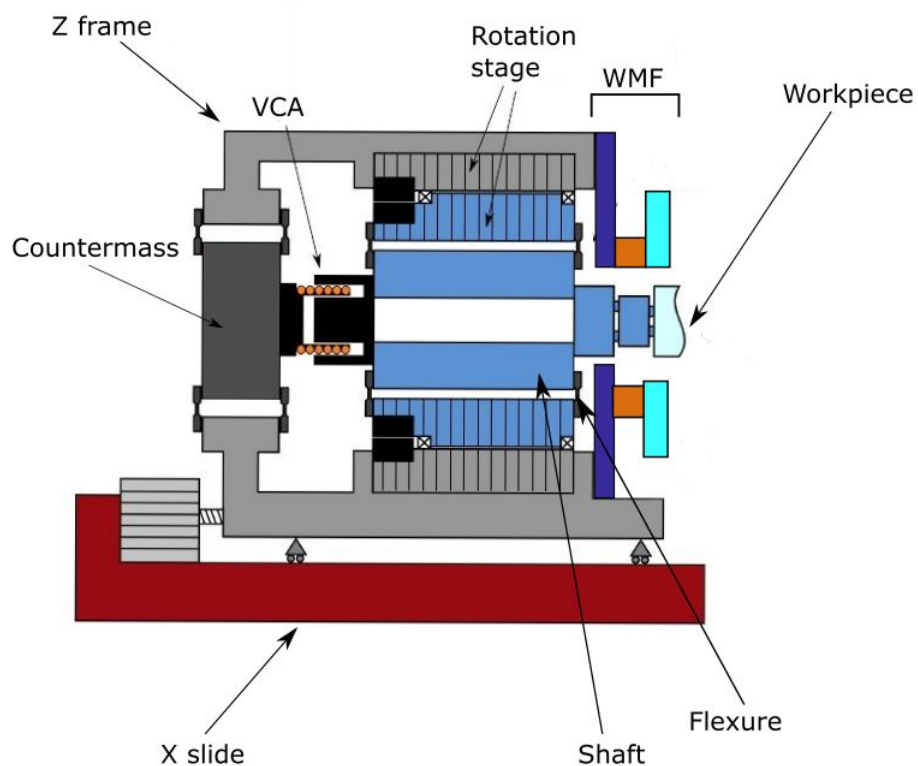
Figure 3.1: Scheme of the different parts of the RLA machine.

The working principle of the RLA is the following. By adding current into the VCA, the shaft displaces into the z-direction. With this displacement, the workpiece can be moved into the desired position. The aim of the VCA is not to position the piece in the whole range of the z-slide, but to eliminate disturbances that can be produced by the grinding forces. It also eliminates another external or internal forces that can be created in the grinding process, as well as other disturbances created by the movement of the machine.
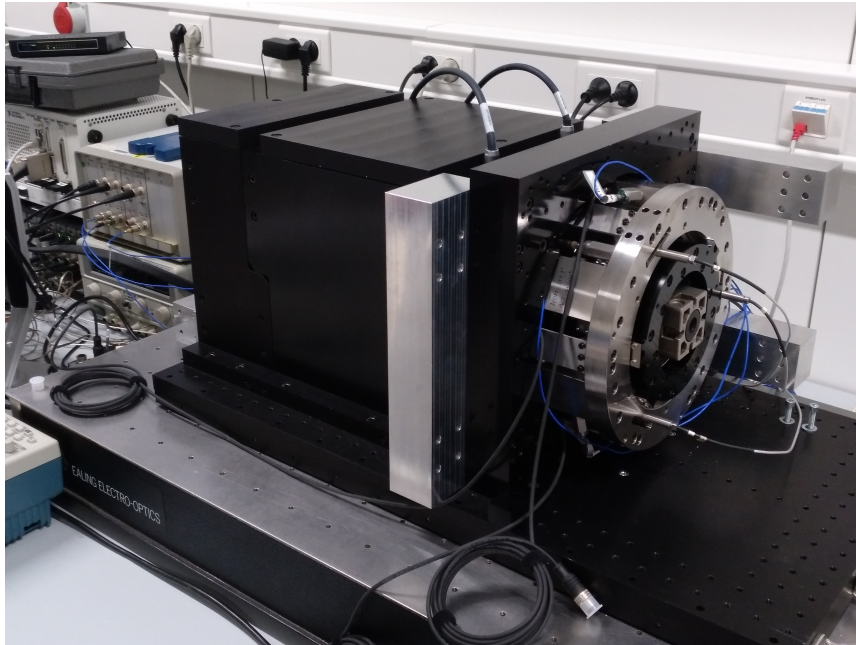
Figure 3.2: Z-frame in its current state.
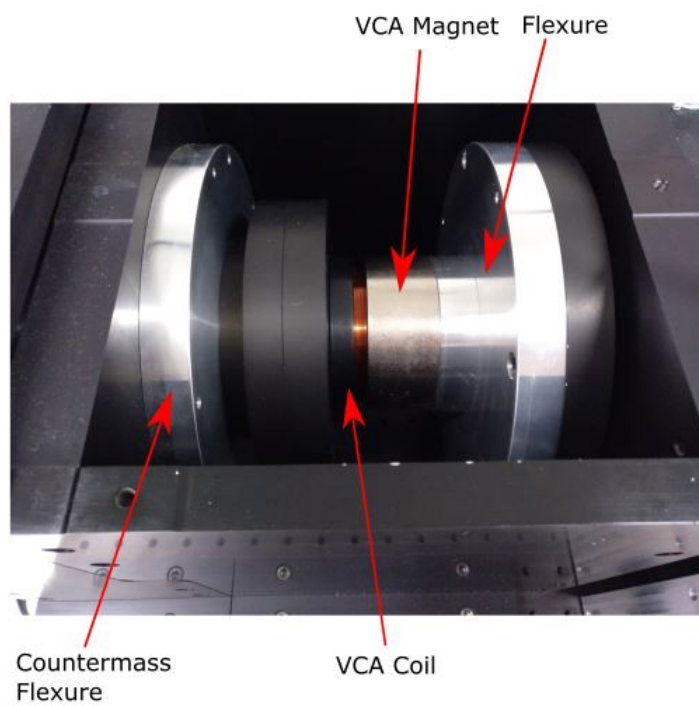
Figure 3.3: The upper part of the RLA opened.

3.2 Mass-spring model

To understand how the system behaves and to get a mathematical model of it, a mass spring damper system is studied. For doing so, a Simscape Simulink from MATLAB is used. Also the values of the different components of the machine are discussed in this part of the chapter. The Simulink model can be seen in the figure 3.4. It also corresponds to the elements that appear in the scheme 3.1.

3.2.1 Explanation of the mass-spring-damper system

As it can be seen, the force of the VCA pushes in between the countermass and the shaft. The shaft is divided in two parts, because as proved in [10], at high frequencies it reaches a mode in which translational movements can be seen. As a consequence of this, the both bigger parts of the shaft can be modelized as two masses with a spring in the middle.

The output that is needed to obtain is the displacement of the metrology frame. For doing so, a set of 3 capacitive sensors has been placed in the reference ring in order to measure the distance from the shaft. Other sensors are also placed in the set-up, for example, the accelerometers in the reference ring. Apart from the sensors, some connections with other elements with the z-frame can be seen in 3.4.

Flexures connect the shaft with the rotatory table and with the countermass. Since the VCA will excite the system into a perpendicular direction of the table legs, the stiffness and damping of the table are also considered. This might have some influence in the process. Despite the fact that this behaviour would not be repeated in the machine, it has to be taken into account while analysing the system.

3.2.2 Parameter values

To get some data, the values of the parameters are assumed by looking into [16] and [10]. Another values can be calculated by assuming damping of 1% . The list of parameter can be shown in the Appendix A.

To calculating the different masses of the shaft, the next formula is used:

$$\omega_n = \sqrt{\frac{k(m_1 + m_2)}{m_1 m_2}} \tag{3.1}$$

being:

$$m_{\text{shaft}} = m_1 + m_2 \tag{3.2}$$
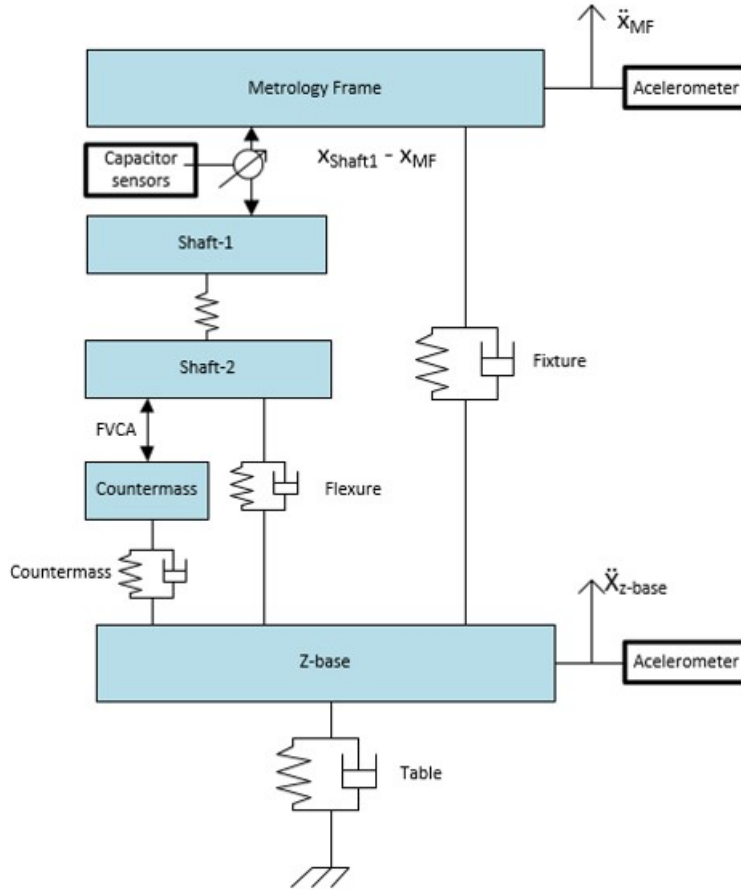
Figure 3.4: Mass spring damper model implemented into Simulink.

and being:

$$m_1 = \alpha m_{\text{shaft}} \tag{3.3}$$

$$m_2 = (1 - \alpha)m_{\text{shaft}} \tag{3.4}$$

Using the values of A and the ω_n from [10] which corresponds to 2570 Hz, a value of the masses of $m_1 = 5.016kg$ and $m_2 = 0.684kg$ has been obtained by solving the system.

The stiffness of the table is also calculated in [11], but the values are not exactly correct, so this stiffness is recalculated in this thesis. The procedure is similar, even thought the measurement used is not the same and it is not also the final value. First, a profile like the one showed in figure 3.5 is been used.

19
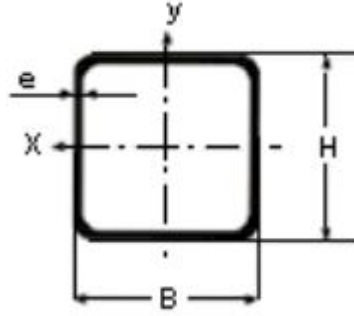
Figure 3.5: Profile of the table leg that is being measured

The measurements of the profile are $50mm \times 50mm$. The height of the table is 90 cm. To calculate the stiffness of the leg of the table, the formula 3.5 has been derived. The inertia momentum is obtained from appendix n entering by "Momento de inercia" and 50×50 with a 2mm (assumed) of thickness of the profile. The material of the table leg is assumed aluminium, so the elastic modulus corresponds to 71 GPa. It has been taken into account that there are 4 legs in the table so since the stiffness is in parallel, it has to be added.

$$k = \frac{4 \cdot 3EI}{L^3} = 0.209201 N/\mu m \tag{3.5}$$

Also a damping of 1% will be assumed using the formula 3.6. This values are also shown in Appendix A.

$$\zeta = \frac{c}{2\sqrt{km}} \tag{3.6}$$

3.3   Simulation results

The model is implemented into Simscape blocks form Simulink MATLAB, in order to obtain the transfer function that shows the displacement in relation which the force as an input of the VCA. The transfer function is shown in figure 3.6. The peaks that can be seen in the picture have to be identified. To do so, the frequency of the effect of the table is calculated. The frequency is obtained by formula 3.7. This formula obtains the frequency in $rads^{-1}$ so diving by 2π is needed to get the value in Hertz.
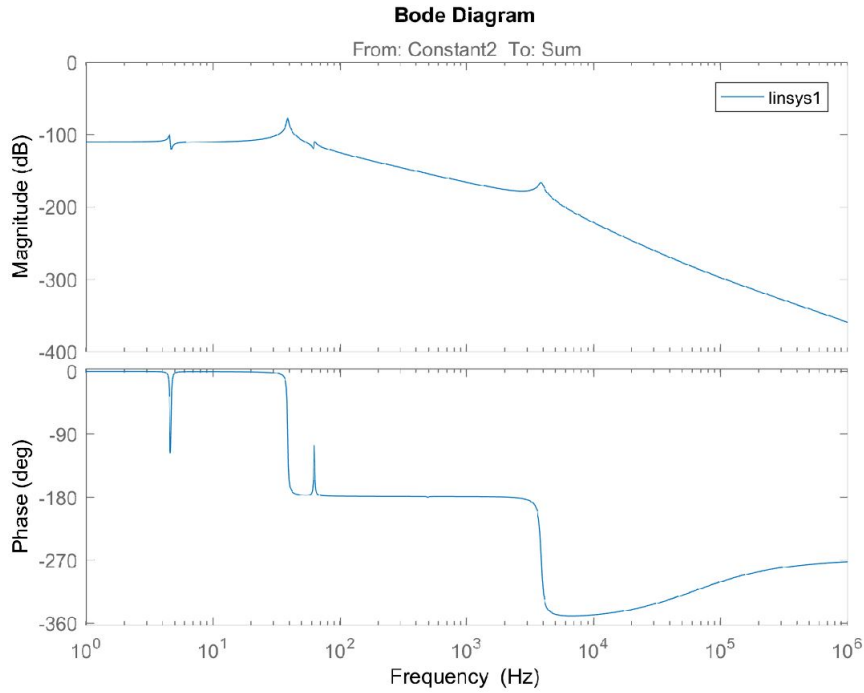
Figure 3.6: Transfer function of the system, analyzed in MATLAB

$$\omega = \sqrt{\frac{k}{m}} = 83.5066 rads^{-1} = 13.29 Hz \tag{3.7}$$

This frequency is not exactly the same as one of the peaks that can be seen in the figure 3.6. The order of magnitude is closer to the first peak than to the third one. For that reason, this peak is assumed to be the one created by the legs of table.

As it can be seen in the figure 3.6, there are several behaviours that need to be studied. First, a resonance anti-resonance peak around 4.5 Hz. This peak has been localized as the one created by the legs of the table. The next peak that can be found is at the frequency of 38 Hz. This frequency is the one that excites the shaft because the axis resonates on the stiffness of the flexure. The next one is an anti-resonance resonance peak in 65 Hz. Since the first belongs to the leg of the table, this one is created by the countermass. This effect might have to be taken into account while analysing the system. The last peak is the one in high frequency at 3.86 kHz.

21

3.4   Conclusion

In this chapter, the working principle of the machine has been explained. The different components of the RLA have been introduced and also their function on the machine. Then, the machine has been modelized using a Mass-Spring-Damper scheme. The scheme has been implemented in Simulink and a transfer function has been obtained as result. By looking at the transfer function, the behaviour of the system can be understood. There are some peaks that could make the control under-perform such as the ones at 65 Hz and the one at 3.86 kHz.

Chapter 4

System Identification

This chapter will approach the identification of the system by means of different experiments performed in the machine. First, the set-up used in order to obtain the values of the transfer function is discussed and explained. Then, the procedure to take the experimental data from the sensors is presented. At last, the final results will be shown and analysed as it will be used towards controlling the system.

4.1   Set-up of the system

To obtain the data, besides the RLA Machine, a data acquisition system is needed. This system requires both electronic devices and software to get the data into the PC. The system used is presented in this section. To understand the connection required by the different elements, as well as the data needed by all of them, the picture 4.1 is presented.
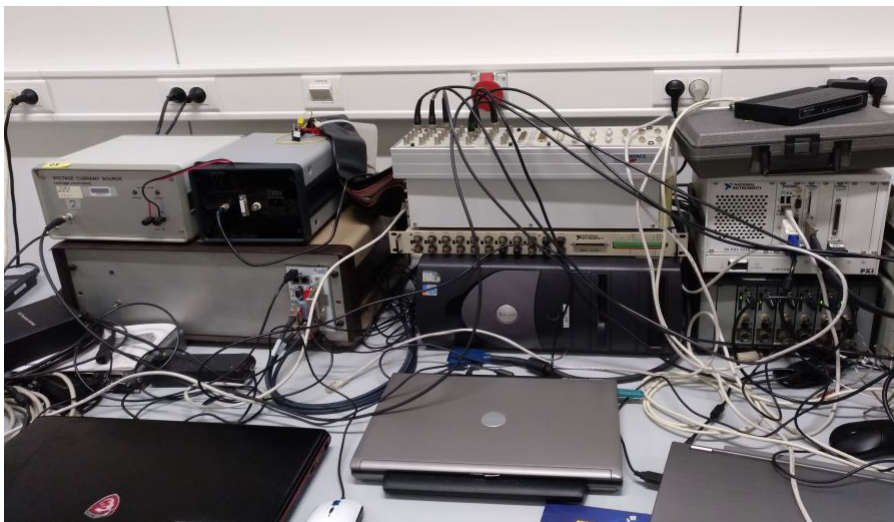
Figure 4.1: Setup of the data acquisition in the lab.

In figure 4.2 the set-up is shown in an scheme to be easily understood.
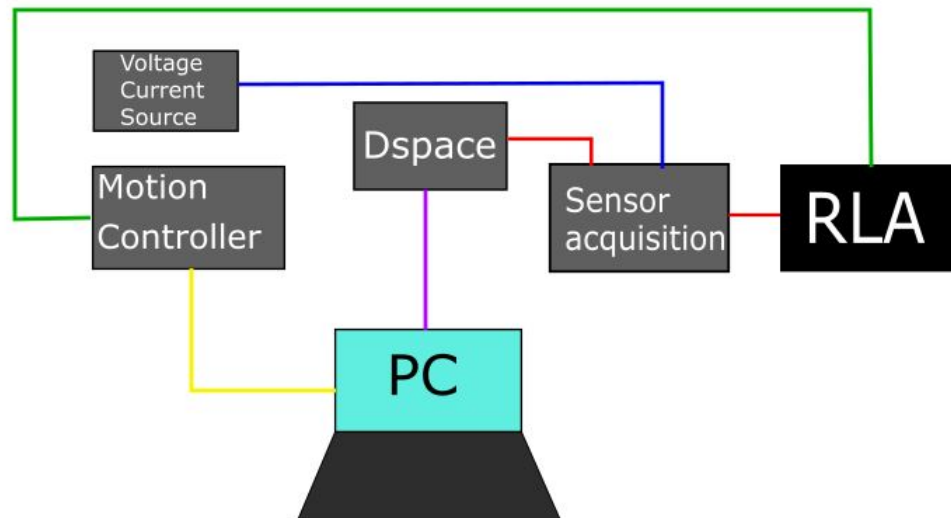
Figure 4.2: Scheme of the data acquisition in the lab.

- The line between the Dspace and the RLa handles the values of the sensors, both capacitor sensors and the accelerometers and also it sets up the value for the VCA. It obtains from Dspace all the information needed, and also it sends the voltage needed to move the VCA in the position desired.

- The line that connects the motion controller and the RLA contains the information related with the rotary stage. It sends the value of the position of the motor from the motion controller and it gets the information from the encoders that are implemented in the machine.

- The line between the voltage source current and the sensor acquisition gives the voltage needed to the sensors. The values cannot exceed the range value of $\pm 2V$ otherwise the voltage source could saturate and break.

- The line that goes from the computer to the PC is the one responsible of communicating the values of the encoders and the motor with the PC. To handle the data, a specific software is required. This software is ComET from ETEL.

- The line between Dspace and the PC belongs to the control of Dspace. With Dspace, the values can be easily used by means of a Simulink model. Both Simulink MATLAB and ControlDesk Dspace need to be used. With Simulink, the scheme of the system can be easily modified and ControlDesk is used to connect with the physical device.

4.2 Identification Procedure

To identify the system, a certain procedure needs to be followed in order to achieve consistent results that can be used for a later controlling of the system. The procedure followed is the next one. A model in Simulink has been built to get the data. In this model, the data of the six sensors available (three capacitor sensors and three accelerometers) has been displayed. Also, the value of the voltage that goes into the VCA has been included in the model.

Given an input signal, the VCA is excited and the system starts to move. The capacitor sensors and the accelerometers measure the displacement and a file of values is saved. This procedure is reproduced by means of both Simulink and Dspace ControlDesk.

The signal that is introduced in Simulink to excite the system is a multisine signal. This signal is created by means of a MATLAB function from the toolbox provided by the course advanced model based control. It requires as an input the sampling frequency and the frequency range. Also, the frequency resolution in which the function is divided. Once the multisine signal is created, it is implemented into the system to get the necessary to the identification.

The identification of the system makes use of two different methodologies, NLLS and ML. Both obtain the data in discrete time and are explained in [20]. The data needed to get the FRF of the system is the one coming out of the three capacitor sensors and from the voltage of the VCA.

4.3 Results of the identification

From the procedure that has been explained, a set of results is obtained in order to achieve the most accurate model of the system. The multisine signal that has been chosen has 50kHz of sampling frequency, since it is the maximum value from which the acquisition system can work properly. A range in between 10Hz and 5kHz has been chosen because there is no interest at controlling the system at higher frequencies. Finally a resolution of 8 Hz is chosen in order to not create a set of data too large. From this point, the signal has been implemented into the system and the values from the data have been obtained.

The first comparison can be done between the FRF acquired from the machine and the one that obtained in 3 as a result of the Simulink model. As it can be seen in the picture 4.3 both transfer functions are close to each other. It differs in high frequencies. Meanwhile in the Simulink model, the peak is at 4kHz, in the system is produced around 2kHz. The gain has been adjusted. It can be seen a phase lag in the process.
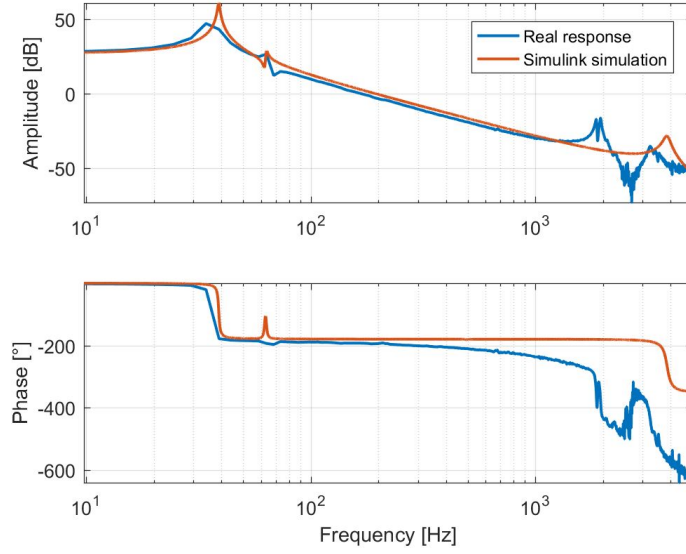
Figure 4.3: Comparison between Simulink model and identified transfer function.

The second comparison that can be done is the one between ML(Maximum Likelihood) and NLLS (Non Linear Least Squares) method. In figure 4.4a and 4.4b it can be seen that the ML fits better into the curve than the NLLS. Because of that, to get the mathematical model the ML method is going to be selected.

(a) Maximum Likelihood Method

(b) Non Linear Least Square
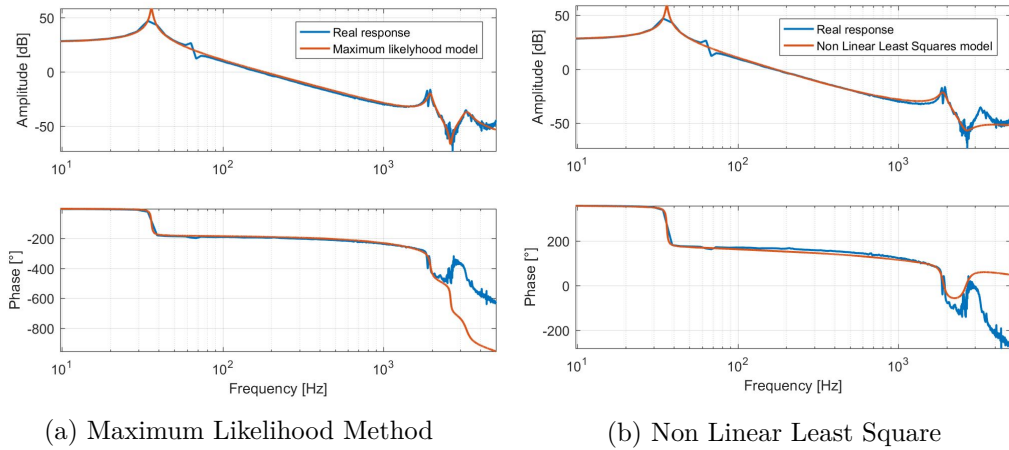
Figure 4.4: Comparison between both methods of identification

In high frequencies, a delay can be seen. The phase plot should remain around -180 degrees (ϕ_e) but it gets -237 degrees (ϕ_r) measured in 1kHz. The phase lag is identified and neglected from the system. The delay is calculated as:

$$\tau = \frac{(\phi_r - \phi_e)}{360 \cdot 1000} = 1.1944 \cdot 10^{-4} s \tag{4.1}$$

Taking into account that the sampling frequency is 50kHz, this means that the delay is approximately 8 time steps. With this delay calculation, the transfer function can be modified as follows:

$$Y_{\text{nodelay}} = Y_{\text{delay}} \cdot e^{i2\pi f_s \tau} \tag{4.2}$$
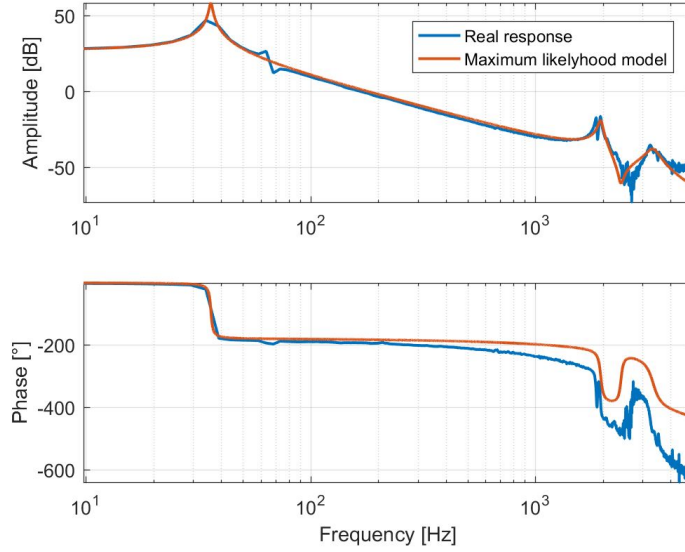
Figure 4.5: Transfer function without delay.

So the poles and the zeros that are used are the ones seen in the table A.1. From now on the system will be treated as a system without delay. The transfer function without phase lag is shown in figure 4.5. In the table it can be seen that there are 2 zeros that might cause some trouble in order to control the system. This both zeros will be treated in the next chapter.

Poles	Zeros
0.466 + 0.815i	0.946 + 0.287i
0.466 - 0.815i	0.946 + 0.287i
0.966 + 0.244i	-0.005 - 0.800i
0.966 - 0.244i	-0.005 + 0.800i
0.999 + 0.005i	
0.999 - 0.005i	

Table 4.1: Poles and zeroes of the system.

4.4 Merged identification

The peak that in the previous chapter is meant to be the effect of the leg of the table is not represented in the identification. To get this peak into the identified model, the whole frequency range is going to be split in two different transfer functions. In the first one, the low frequency peaks are going to be obtained, so the range is from 10Hz to 100Hz with a resolution of 2Hz. The second one is from 100Hz to 5kHz in order to evaluate the high frequency peaks. It can be seen in figure 4.6. The fact that the lag has been taken out has to be taken into account when analysing the similarities in the high frequency plot.

(a) Identification at 10Hz and 100Hz   (b) Identification at 100Hz and 5000Hz
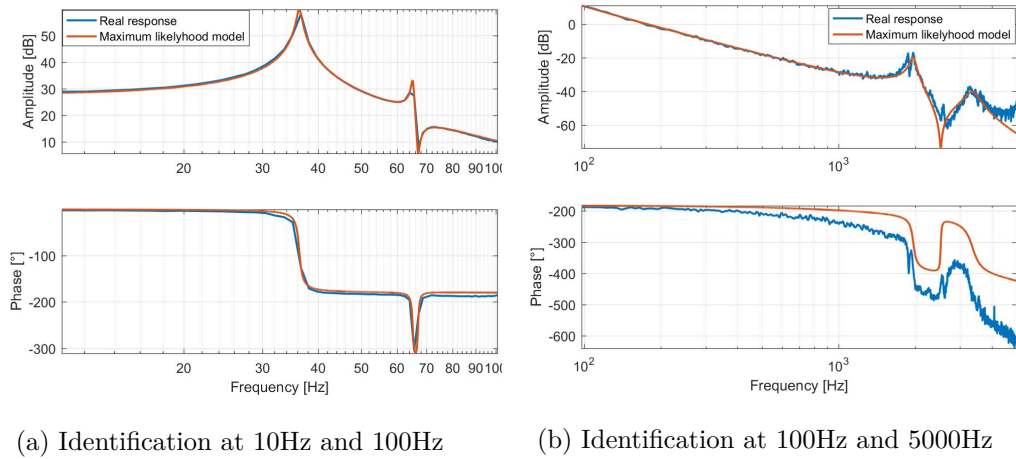
Figure 4.6: Identification Split

The problem is that both transfer functions cannot be added. To solve this problem, both transfer functions are going to be transformed to eigenvalues and eigenvectors. The first step is converting the function to state space. This is done with MATLAB. State space representation can be seen in:

$$\begin{cases} \dot{x} = Ax + Bu \\ y = Cx + Du \end{cases} \tag{4.3}$$

Then the state space system has to be transformed to eigenvalues and eigenvectors. MATLAB is used to perform this transformation. The procedure can be seen also in [6]. The eigenvalues matrix E and the corresponding eigenvectors matrix V are obtained. The transformation is done as follows:

$$\begin{cases} \dot{q} = V^{-1}AVq + V^{-1}Bu \\ r = CVq + Du \end{cases} \tag{4.4}$$

It just remains to add both transfer functions, taking into account that the order of both together has to be achieved. The order of the system is $n_1 + n_2$ which in this case is $4 + 6 = 10$ .The result can be seen in picture 4.7.
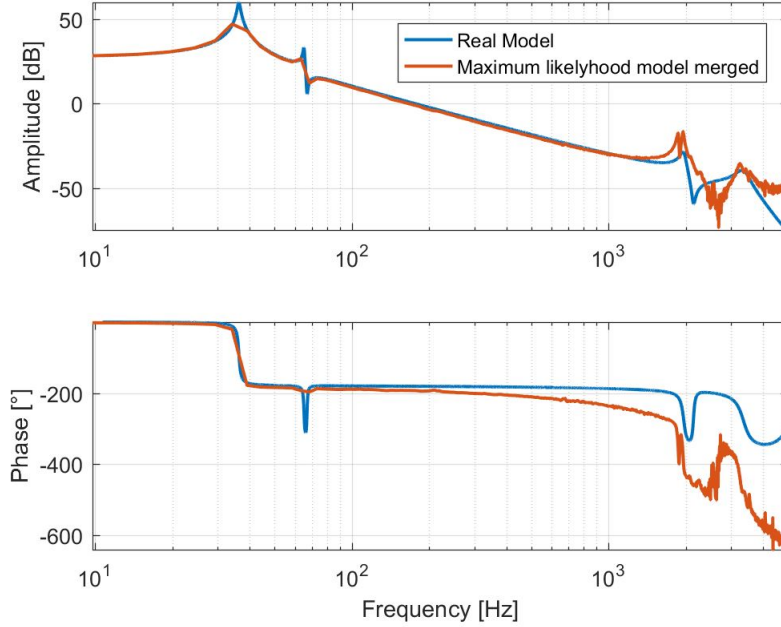
Figure 4.7: Merging of 2 transfer functions into one.

As a final remark, this merged transfer function are used at the end as the final representation of the system. This is because the peak that could not appear in the first case is the one that correspond to the countermass. This peak appears in the RLA system, but from now, it is not used to not add extra complexity to the model. From the control point of view, if the controller bandwith is around 100 Hz or less, this peak has to be taken into account. Nevertheless, this procedure has not be done in vain. It will be used along the thesis in some other chapters.

4.5 Conclusion

Some conclusions can be drafted from the development of this chapter. An introduction about the system of the acquisition data has been done, identifying every element and describing the function that performs into the system. An explanation of the procedure of acquisition data has been performed, both explaining the mathematical and the procedure realized on the computer. A review about the results has been displayed. Also, the results has been modified in order to have a better control of the system. Finally, a deeper identification of the system has been performed and the procedure to transform and get the eigenvalues has been introduced.

Chapter 5

PID Design

In this chapter, the design of a PID Controller (Proportional Integral Derivative Controller) is described. The first part analyses in depth the transfer function obtained in Chapter 4. An adaptation to the system in order to make it more suitable to the PID design follows. As a solution to some of the problems encountered, a design of notch filters is going to be explained. The last part is an analysis of the results obtained by the procedure.

5.1 Transfer Function Analysis

At first, an analysis of the transfer function is done in order to determine the problems that might appear when designing the PID controller. To recall, the figure 5.1 shows the transfer function of the system that needs to be controlled.
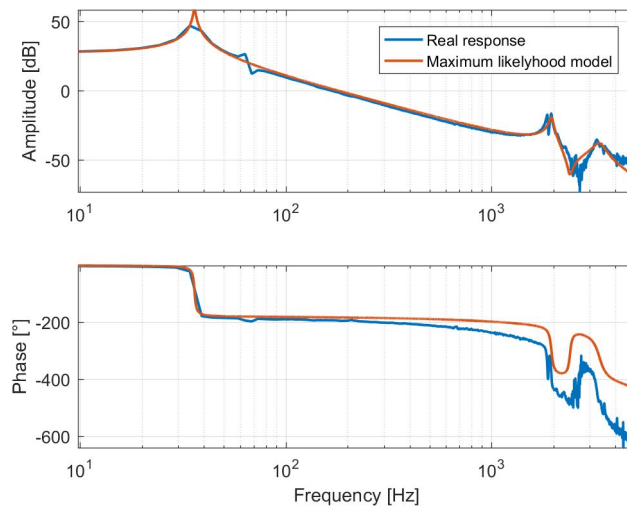
Figure 5.1: Transfer function without delay.

While looking at the transfer function, it is noticed that the delay has been taken out of the system. The next step that is an analysis of the poles and the zeros of the system. To do so, a MATLAB function is used and so, the poles and the zeros can be seen in figure 5.2.
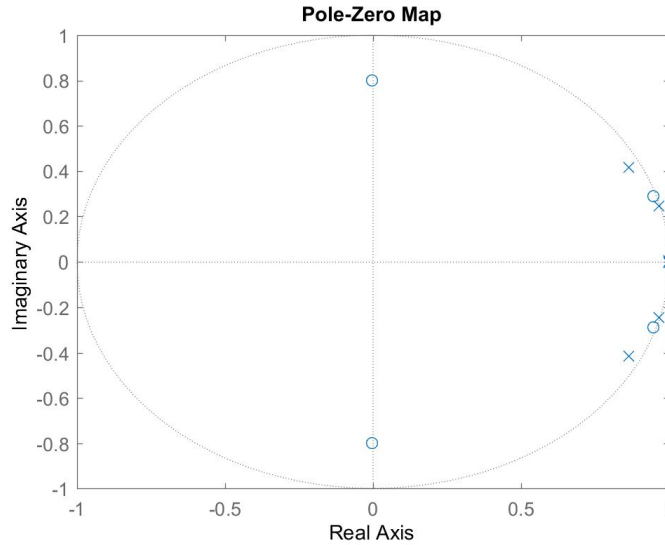
Figure 5.2: Poles and zeros of the system.

The poles-zeros map shows that all zeros and poles belong inside the unit circle. Due to this fact, the system is stable. Nevertheless, two zeros are located in really high frequency (12.7 kHz). Since those zeros are not interesting and can add instability to the system, they are going to be removed from the model. Since the model is just a mathematical representation of the system, it might not be a accurated to remove the zeros because in the real system they will be still there. But if they are correctly identified, an appropriate filter can be designed in order to prevent the zeros from disturbing the system.

To do so, the poles and the zeroes have been identified with a MATLAB function, and a new system without the zeroes has been created. The zeros at 12.7 kHz have been eliminated and also the gain has been multiplied by the inverse of the poles as shown in formula 5.1:

$$K = \frac{1}{(1 - z_1)(1 - z_2)}$$ (5.1)

The difference between the two transfer functions can be seen in figure 5.3.
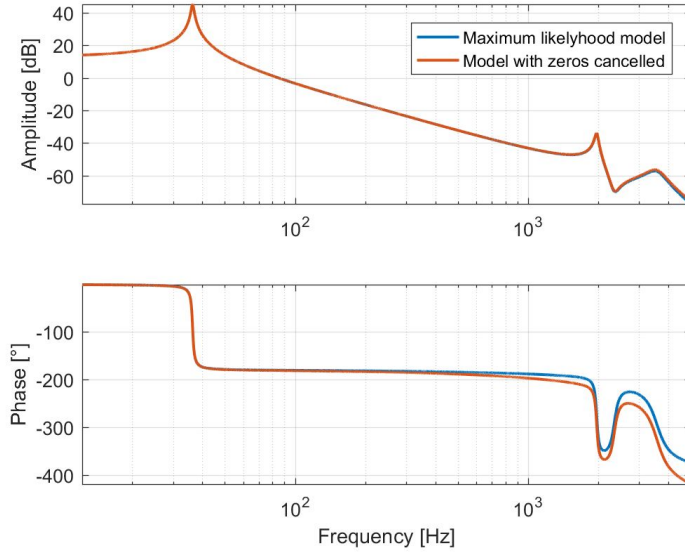
Figure 5.3: Transfer function with two zeros cancelled.

5.2 Notch Filters

To deal with the high frequency peaks, some filtering can be applied. Notch filters can be used to soften the high frequency peaks. The function of the notch filters is to reduce the gain of a certain frequency. The transfer function of the notch filters can be seen in 5.2. The design of the notch filters is done as in [7]. So first, the frequencies of the peaks need to be determined, and then the rest of the values will be tuned by hand. The values of the frequencies are 1980 Hz and 3520 Hz.

$$H(s)_{\mathrm{nf}} = \frac{s^2 + 2a\omega_0 + \omega_0^2}{s^2 + 2b\omega_0 + \omega_0^2} \tag{5.2}$$

Before tunning the notch filters, the results are the next ones:

For the first notch filter, $\omega_0 = 2\pi 1980 \, rad \cdot s^{-1}$, $a = \frac{0.07}{2}$, $b = \frac{1}{2}$

For the second notch filter, $\omega_0 = 2\pi 3520 \, rad \cdot s^{-1}$, $a = \frac{0.2}{4.422}$, $b = \frac{1}{4.422}$

Once the filter has been designed, as it has been designed in s-domain, it has to be converted to z-domain using the MATLAB conversion to discrete, so the notch filters will remain as follows:

$$H(z)_{\mathrm{nf1}} = \frac{0.9463z^2 - 1.827z + 0.9382}{z^2 + 1.827z + 0.8848} \tag{5.3}$$

$$H(z)_{\mathrm{nf2}} = \frac{0.9636z^2 - 1.731z + 0.9454}{z^2 + 1.731z + 0.909} \tag{5.4}$$

Figure 5.4 shows te comparison between the transfer function with the notch Filters included and the one without the notch filters. The peaks in high frequency has been softened. Nevertheless, a huge phase delay is also present in the bode plot. This phase delay could make the control really hard to implement since it will decrease the PM (Phase Margin) that can be applied to the controller. The behaviour of the Notch Filter in the control scheme is discussed in the following sections of this chapter.
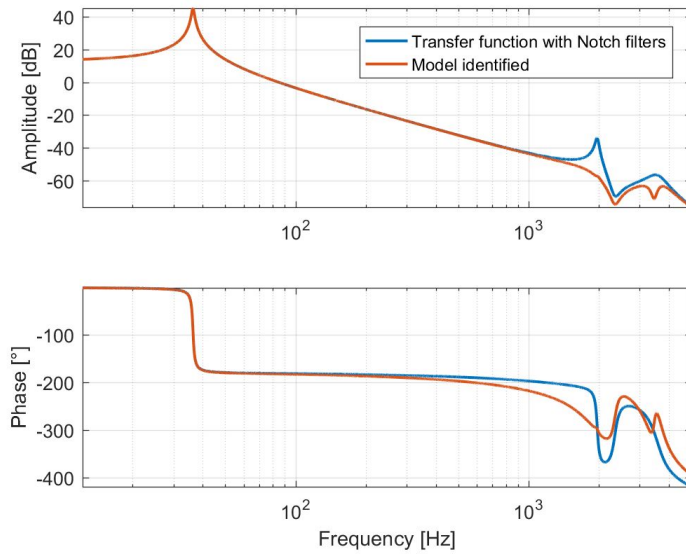
Figure 5.4: Transfer function with the Notch filters implemented.

5.3 PID Design

A PID controller is going to be designed first. The reason to choose PID instead of just a Proportional or a Proportional Integrator controller is because the Derivative action is needed in order to make the response faster. Also the Integrator is needed since the aim is to get the tracking error as low as possible in the machining process. Since there are a lot of procedures to design a PID, the one from [18] is selected. Since the results can change depending on the transfer function selected, the procedure is implemented in a MATLAB code. The steps will be shown in order to achieve the final controller.

The first step is select the α value to achieve the maximum lead at 55° This value is chosen to achieve a compromise between maximum PM and amplification of high frequencies, which is one of the main problems of the system.

The second step is, chosen a PM, to look for the value of the frequency in which the gain will have a value of:

$$\phi = -180° + PM - 55° \tag{5.5}$$

Next, the maximum frequency will be used to calculate the break frequency of the lead compensator as follows:

$$T = \frac{1}{\omega_{\max}\sqrt{\alpha}} \tag{5.6}$$

Since the system is contained in z-domain and the design of the PID controller is done in s-domain, some transformations need to be used. Using the appropriate transformation, the lead controller designed so far is described by formula 5.7.

$$D(z) = \frac{z - \frac{T_s}{T}}{z - \frac{T_s}{\alpha T}} \tag{5.7}$$

The next step is to calculate the integral time. To do so, formula 5.8 is applied.

$$T_i = \frac{\tan(90° + \phi_{\mathrm{PI}})}{\omega_C} \tag{5.8}$$

T_i is also transformed into z-domain. The last step is to compute the gain K. The value of K is the one that makes the close loop gain 1 with the desired PM. The final function of the PID is the one that can be seen in formula 5.9. This function is in discrete time and the expression is the one as follows:

$$D(z) = K\frac{(z - \frac{T_s}{T_i})(z - \frac{T_s}{T})}{(z - 1)(z - \frac{T_s}{\alpha T})} \tag{5.9}$$

Using this procedure, a PID has been designed. The transfer function of the PID is the one that can be seen in figure 5.5 that corresponds to a typical bode plot of a PID.
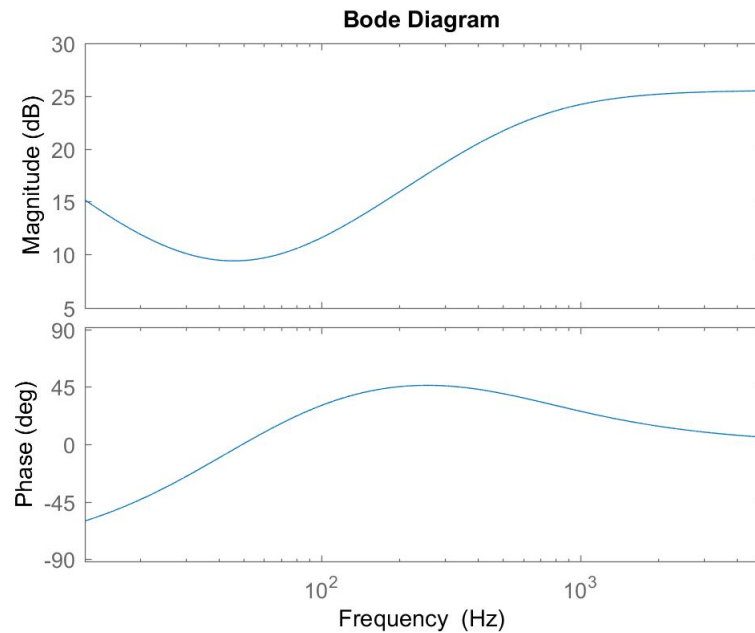
Figure 5.5: Bode plot of the PID Controller.

5.4 Results of the PID Controller

Once the procedure of the PID has been designed, the values from the model have to be implemented in order to control the system that used. Since a PM of 45 was not sufficient to achieve an stable control, this PM has been decreased first until it reaches an stable value. Decreasing the value of the PM will result in an slower time response.

To obtain results, different models have been simulated. The first comparison that is done is the effect of the suppression of the zeros. It has been done in order to determine whether the suppression does affect at the controller at the end. To establish the comparison, similar conditions have to be assume in both cases. The PM has set to 42° and the delay of the PI has been set to 10°.
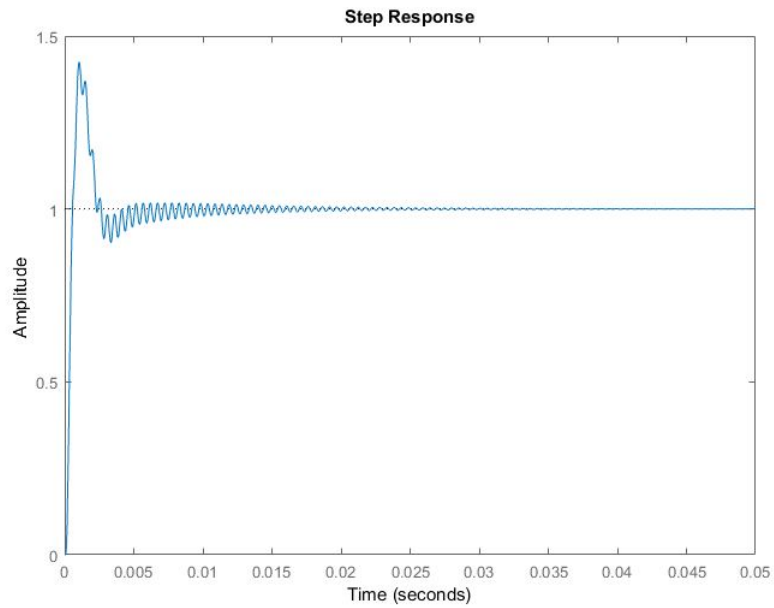
Figure 5.6: Step input of the system.
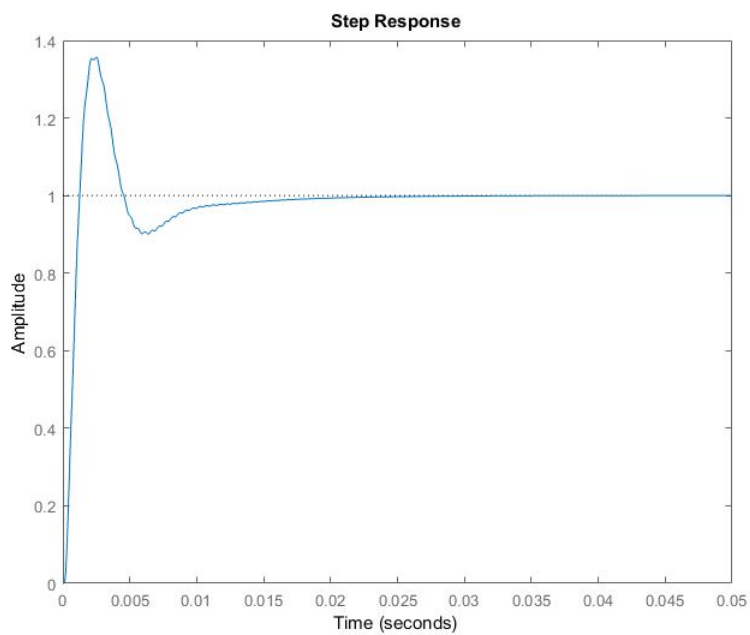
Figure 5.7: Step input of the system with the two zeros cancelled.

Looking at figures 5.6 and 5.7 two characteristics can be seen. The first one is how

the step input behaves. In the non modified signal, the response is curly, comparing to the one modified. This modification allows fast settling time, since the system will not oscillate that much. The second is the settling time. The model without any modification is much faster than the modified. This is due to the phase delay that can be seen between the two models. Nevertheless, since it was a delay in the system that was neglected first, further actions will be taken in order to deal with the delay in the system.

The next simulation that is the use of the notch filter within the system. The simulation needs to be performed in order to evaluate whether the use of the notch filters will improve the control. An step input has been applied with the same characteristics than were selected. Step response of the system with notch filters can be seen in figure 5.8.
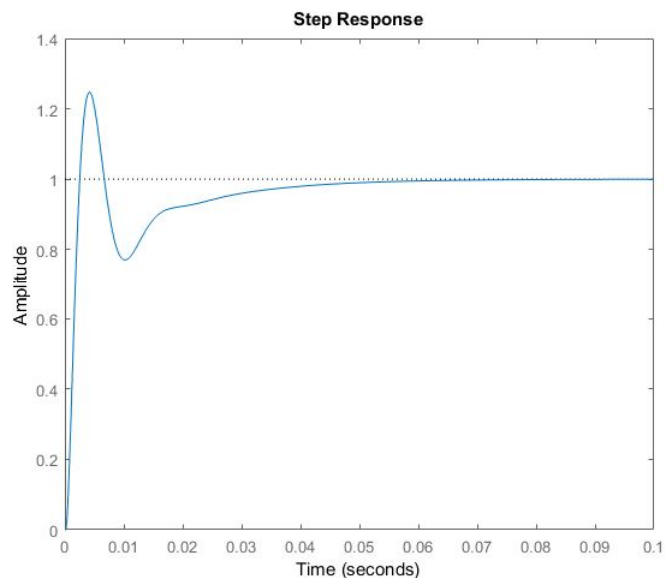
Figure 5.8: Transfer function with the notch filters on.

Looking at the time scale, the time axis is 0.1 seconds while the previous ones were 0.05, it can be seen that the control is slower than before. That is due to the delay introduced by the Notch Filters. For this reason, the solution of putting notch filters to go further in frequency can not be the best solution, even thought they would be tried.

The control PID selected corresponds to the model with the zeros cancelled and 40 degrees of PM. The OL transfer function can be seen in figure 5.9 With this controller, 307 Hz can be achieved. According to [11] this bandwidth is not sufficient to achieve the desired performance, so another strategy of control has to be taken.
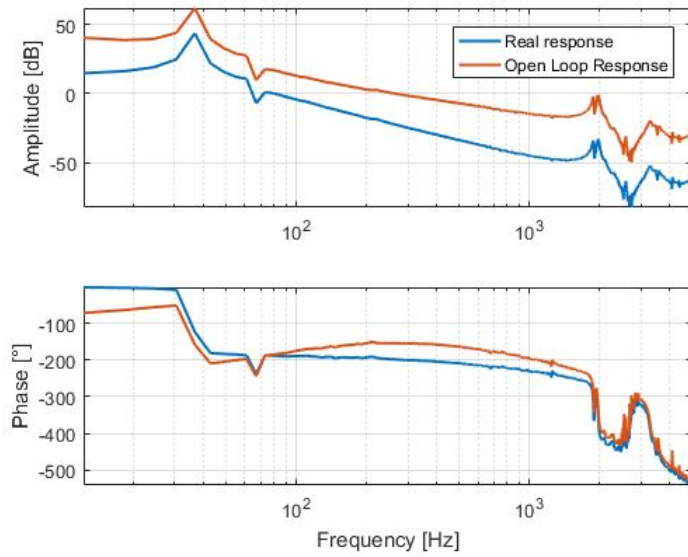
Figure 5.9: Close loop of the system with the PID implemented.

The last simulation is include the phase lag in order to see how much the performance of the controller is decreased. To do so, a Simulink model with the model and the PID data but with the delay calculated as in last chapter is presented. The figure 5.10 represents this comparison.
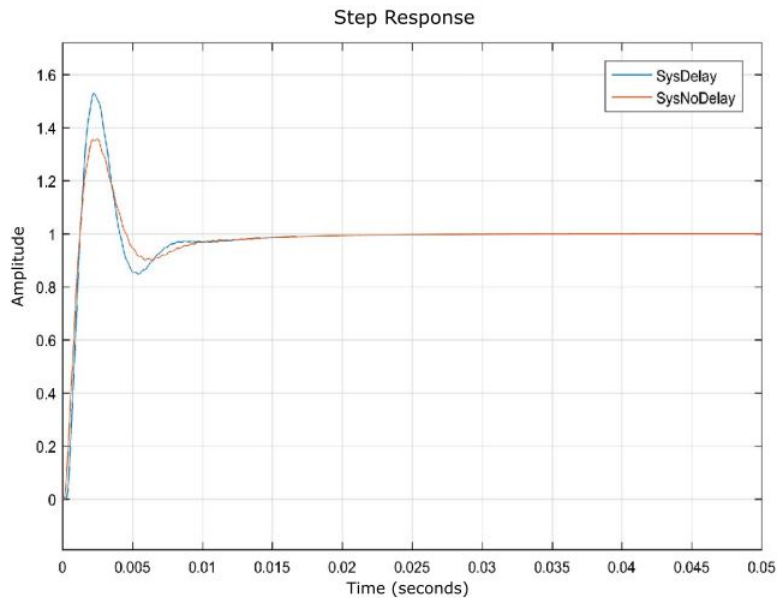
Figure 5.10: Comparison of the system with and without delay.

The model without delay has less overshoot compared to the one with delay. That proves that with the delay included, the control has worse performance than the one calculated earlier.

5.5 Conclusion

A deeper analysis of the transfer function of the model has been performed. By means of this analysis, the way in which the performance of the control might be reduced has been identified and addressed. Two notch filters have been designed in order to have a control above higher frequencies. The design of the PID has been mentioned, explaining the steps needed in order to achieve the best parameters of the PID. The last part of the chapter treated the different responses of the controller, by running different simulations with different control strategies. The PID controller does not reach the specifications needed at the end, so other control strategies are required in order to achieve better results.

Chapter 6

State Space Control

In this chapter, a design of the controller in state space is performed. The first step is to obtain the system in state space. Then, the control law and an estimator need to be designed to achieve the control loop. Next, a modal cancellation has been performed to try to achieve faster control in high frequencies. It follows the way of compensating the error due to the delay that exists in the system. To finish, a set of results and simulations are shown to analyse whether this kind of control is better than the PID.

6.1   System in State Space

At the end of chapter 4, state space had been mentioned to merge two transfer functions. In this chapter, state space is used to design the control. First, the transfer function needs to be transformed to space state matrices. To do so, a Matlab function is been used.

$$\begin{cases} \dot{x} = Ax + Bu \\ y = Cx + Du \end{cases} \tag{6.1}$$

In formula 6.1 State Space system is represented. The matrices are set into canonical form, which makes them more easy to evaluate. The values of the A, B, C and D matrices are shown:

$$A = \begin{bmatrix} 5.6604 & -13.5723 & 17.6556 & -13.1487 & 5.3176 & -0.9127 \\ 1 & 0 & 0 & 0 & 0 & 0 \\ 0 & 1 & 0 & 0 & 0 & 0 \\ 0 & 0 & 1 & 0 & 0 & 0 \\ 0 & 0 & 0 & 1 & 0 & 0 \\ 0 & 0 & 0 & 0 & 1 & 0 \end{bmatrix}$$

$$B = \begin{bmatrix} 1 & 0 & 0 & 0 & 0 & 0 \end{bmatrix}^{\mathrm{T}}$$

$$C = \begin{bmatrix} 0 & 0.0763 & -0.1437 & 0.1221 & -0.0918 & 0.0478 \end{bmatrix} \cdot 10^{-4}$$

$$D = \begin{bmatrix} 0 \end{bmatrix}$$

With those matrix, the transfer function is defined.

6.2   Control Law and Estimator design

Once the system is identified, the control scheme has to be implemented to make the system follow the reference. The control scheme is different than the one used in a PID controller. A scheme of a state space controller can be seen in figure 6.1 obtained from [18]. In this scheme, the Control Law gain (K) and the estimator can be seen. The design and the function of both concepts are explained.
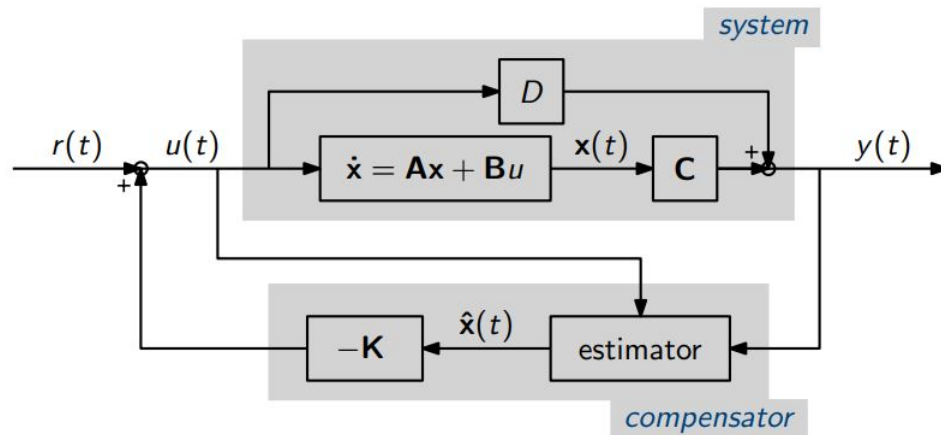
Figure 6.1: Scheme of the state space controller.

The Control Law is the responsible of placing the poles in the place that they should be in order to achieve the specifications of the controller design. The K matrix is the one that contains the information of how to get the poles of the system to where they belong. For this reason, the first step is to design the place of the poles in the z-domain. To do so, there are some methods that can be applied. In this thesis, a method called ITAE (Integral of Time-weighted Absolute Error) is used. This method calculates the pole placement from the frequency needed. The values have

been extracted from a Chinese Journal [4] cited by a MATLAB blog. Since the system is a 6th order system, the 6th order coefficients have been used:

$$s^6 + 2.137\omega_n s^5 + 5.616\omega_n^2 s^4 + 6.902\omega_n^3 s^3 + 6.777\omega_n^4 s^2 + 3.733\omega_n^5 + \omega_n^6 \qquad (6.2)$$

This poles are designed in s-domain, so a conversion to z-domain is needed. This conversion can be done with formula 6.3.

$$p_d = e^{T_s p_c} \qquad (6.3)$$

Poles are already designed. It is left to determine the K matrix. To do so, the MATLAB function "place" is used. The value of the K matrix calculate can be seen:

$$K = \begin{bmatrix} 0.7346 & -3.3070 & 6.0839 & -5.7139 & 2.7384 & -0.5355 \end{bmatrix} \qquad (6.4)$$

A FF (FeedForward) controller is designed to correct the steady state error. The FF controller makes the reference to be followed by adjusting the gain to the right value. To do so, the output value of the state space controller has to be compared with the value of the reference, so a gain equal to the reference divided by the output would be added. In this case, the FF is equal to 412.0548. An step response of the controller can be seen in figure 6.2.
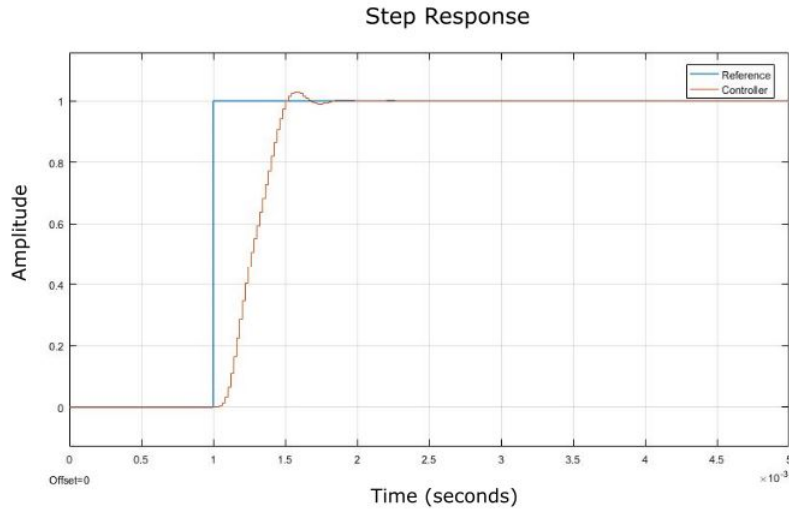
Figure 6.2: Response of the system with the control law implemented

Nevertheless, since all the six states that the State Space model cannot be measured, an estimator needs to be designed. The scheme of the estimator can be seen in figure 6.4. So what needs to be designed is the value of the L matrix. In order to determine

this value, according to [18] it suffices to place the poles 5 times faster as the control law. It also requires to convert the poles to z-domain. The response of this controller can be seen in figure 6.3.   The problem is an error in steady state that appears into
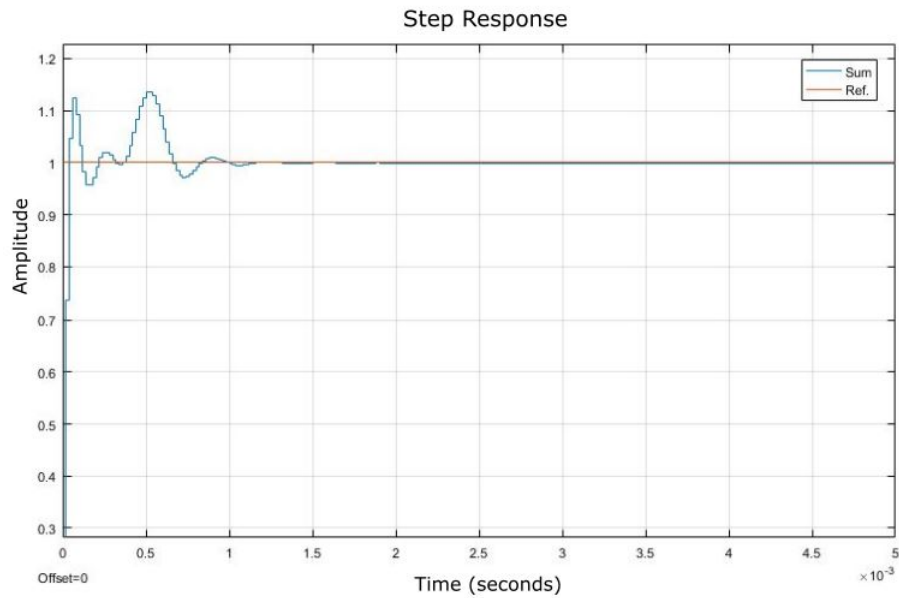
Figure 6.3: Response of the control law and the state estimator.
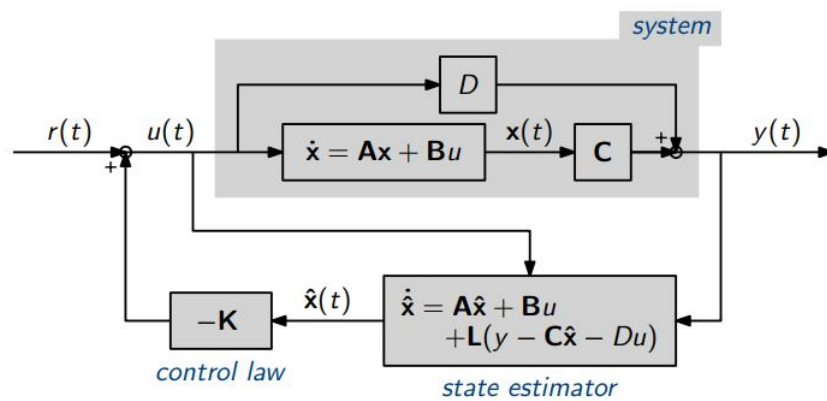
Figure 6.4: Scheme of the state space controller with the equation of the estimator.

the system. This error is 0.055% of the value of the step input. The effect of this value is discussed afterwards.

44

6.3 Modal Filtering

As it was mentioned in the introduction, a main problem that appears in the system is the high frequency peaks produced by the ball bearings. In this section, the effect of the ball bearings neglected by means of a modal filtering.

The modal filtering uses the State Space matrices to neglect those high frequency peaks and get a cleaner transfer function in which the control can go further in frequency. If the filter does work, the effect of the bearings do not dissapear from the system, it is just ignored by the controller. The logic behind this method is that the effect of the bearings cannot be controlled, so by ignoring it, the control can go higher in frequency. In order to use the modal filter, a procedure similar to the one applied in chapter 4 is used. Based on the State Space system described in 6.1, a transformation in the system described in the chapter 4 is performed. The form of the system transformed into eigenvalues can be seen in 6.5

$$\begin{cases} \dot{q} = V^{\text{-}1}AVq + V^{\text{-}1}Bu \\ \quad r = CVq + Du \end{cases} \tag{6.5}$$

The matrix that is transformed into eigenvalues is the Matrix A. The Transformation is performed as $V^{-1}AV$. The values can be shown in 6.6.

$$V^{\text{-}1}AV = \begin{pmatrix} 0.865+0.415i & 0 & 0 & 0 & 0 & 0 \\ 0 & 0.865-0.415i & 0 & 0 & 0 & 0 \\ 0 & 0 & 0.966+0.244i & 0 & 0 & 0 \\ 0 & 0 & 0 & 0.966-0.244i & 0 & 0 \\ 0 & 0 & 0 & 0 & 0.999+0.005i & 0 \\ 0 & 0 & 0 & 0 & 0 & 0.999-0.005i \end{pmatrix} \tag{6.6}$$

In this matrix, the poles are in z-domain. The values of the frequency of each pole are needed to be obtained. Using the formula 6.7 the frequencies of each pole can be obtained.

$$f = \frac{ang(V^{\text{-}1}AV)}{2\pi} \cdot f_s \tag{6.7}$$

The matrix that yields at applying the formula is the one that follows:

$$V^{\text{-}1}AV = \begin{pmatrix} 3562.5 & 0 & 0 & 0 & 0 & 0 \\ 0 & -3562.5 & 0 & 0 & 0 & 0 \\ 0 & 0 & 1973.1 & 0 & 0 & 0 \\ 0 & 0 & 0 & -1973.1 & 0 & 0 \\ 0 & 0 & 0 & 0 & 36.3 & 0 \\ 0 & 0 & 0 & 0 & 0 & 36.3 \end{pmatrix} (Hz) \tag{6.8}$$

Being V the matrix of eigenvectors. As it can be seen, the first 4 modes are the ones that belong to the high frequency peaks, so those four are the ones that need to be suppressed. The way in which the modes are going to be neglected from the system is not from A matrix but from the output matrix which is matrix C. An identity matrix

is created and the 4 first values which correspond to the high frequency peaks are set to 0. This matrix will be named as I_{FIL}. Afterwards, the C matrix is multiplied by this identity matrix so the first 4 values of the C matrix are set to 0.

$$C_{\text{NEW}} = \begin{pmatrix} 0 & 0 & 0 & 0 & 0 & 0 \\ 0 & 0 & 0 & 0 & 0 & 0 \\ 0 & 0 & 0 & 0 & 0 & 0 \\ 0 & 0 & 0 & 0 & 0 & 0 \\ 0 & 0 & 0 & 0 & 1 & 0 \\ 0 & 0 & 0 & 0 & 0 & 1 \end{pmatrix} \cdot C = \begin{bmatrix} 0 & 0 & 0 & 0 & -0.0918 & 0.0478 \end{bmatrix} \cdot 10^{-4} \quad (6.9)$$

Recomputing the value of the system with the new C matrix, the transfer function looks as in figure 6.5.
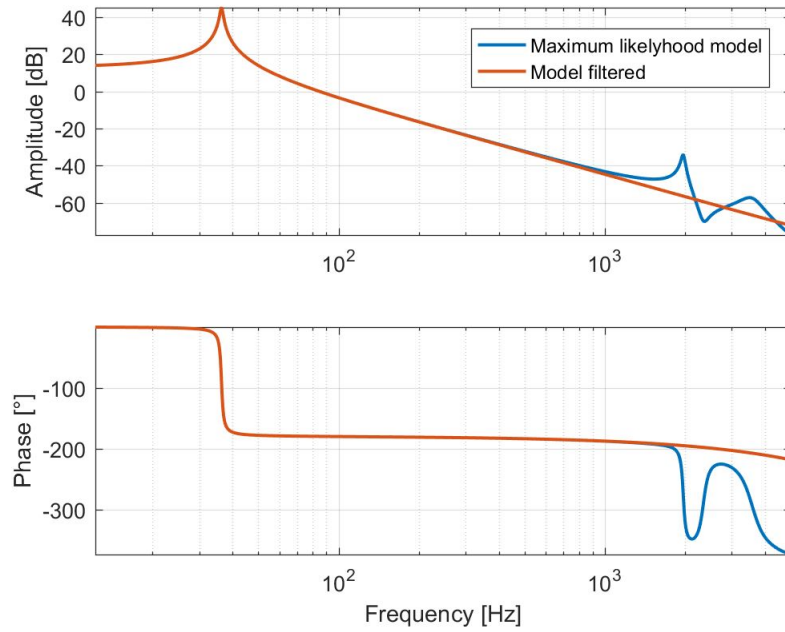
Figure 6.5: Frequency response of the system with the eigenmodes cancelled

This filter works in the frequency domain but it does not work in z-domain. For this reason, a transformation of the filter needs to be performed. This transformation looks like the one shown in formula 6.10

$$C_{\text{TRANS}} = CVI_{\text{FIL}}V^{-1} \quad (6.10)$$

This transformation allows the filter to be implemented into simulink easily by just adding a block with a gain.

6.4 Time delay compensation

One of the main problems encountered during the analysis of the system is the time delay that appears due to the acquisition system. The effect of the time delay cannot be taken out of the response, but the effect in the close loop can be compensated. The solution proposed in this thesis is an estimator called the Smith Predictor. The Smith Predictor is a method that has existed for the past 60 years. It has been explained in books like [21].

There are different configurations in which this predictor can be implemented.
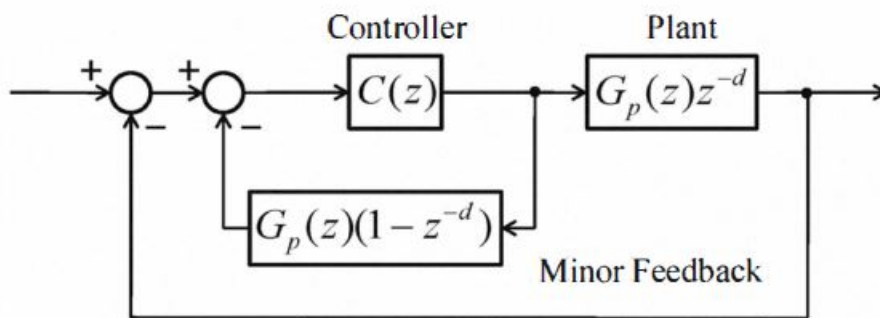

Figure 6.6: Scheme of the Smith predictor

The goal of this predictor is to take out the effect of the delay in the CL by adding an anti-delay in the control Loop. In picture, 6.6 the scheme of the Smith Predictor can be seen. The Smith Predictor has been implemented into Simulink in the scheme shown in figure 6.7.
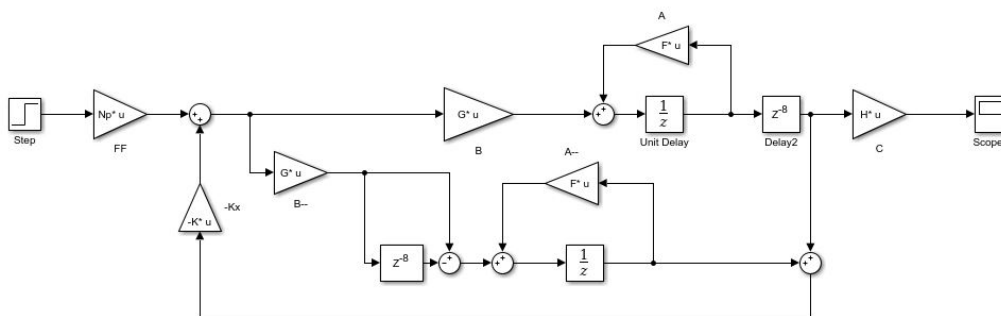

Figure 6.7: Smith Predictor implemented into Simulink

6.5 Simulations

To choose the best scheme of control towards the machine, a set of different simulations with Simulink block are performed. Also the modal filtering is used to perform some of the experiments that need to be done, to measure how good is to neglect the high frequency poles. The first step is comparing the influence of the time delay into the system. The block diagram is represented in figure 6.9. The response of the system has been drawn in figure 6.8. As it can be seen, the delay of the system without the delay compensation leads the system to be unstable while the Smith predictor can compensate the effect of the delay keeping it stable.
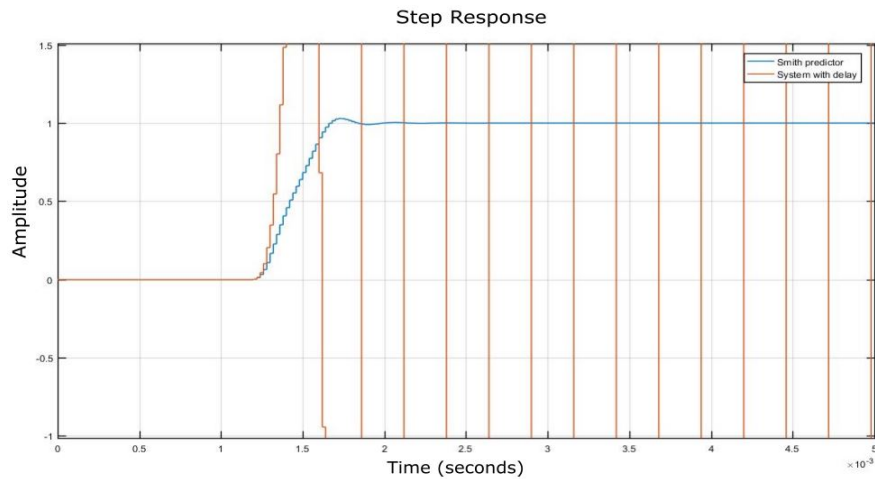
Figure 6.8: Response of an step input with and without delay compensation

Since the estimator needs to be included, the Smith predictor needs to be integrated in the process because otherwise the system would be unstable again. At the end, the space state scheme with the Smith predictor could not be implemented. For this reason, since the delay cannot be corrected, the control of the system by means of the state space is likely to not be achieved.

The scheme with the estimator without the Smith predictor in Simulink is presented in figure 6.10. Besides the estimator, the filter has been also implemented. The filter has a gain equal to $CVI_{\mathrm{FIL}}V^{-1}$ and can be used in case that the Smith predictor is finally implemented. This scheme is presented because even if the response of the system is unstable, it can be helpful for further research. The state space control is tested in the machine to see if it can offer results.
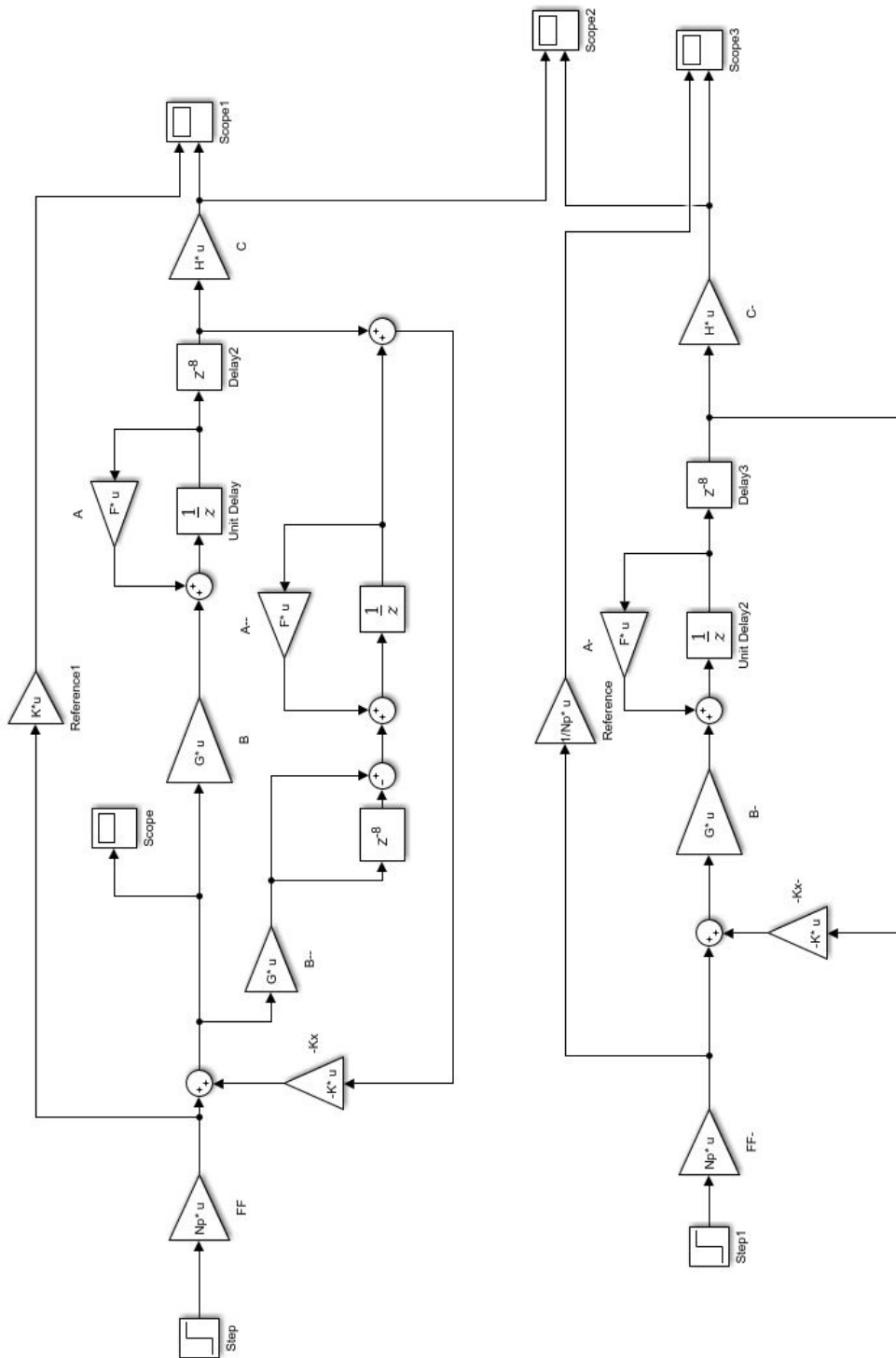
Figure 6.9: Comparison between the control law with and without the Smith predictor
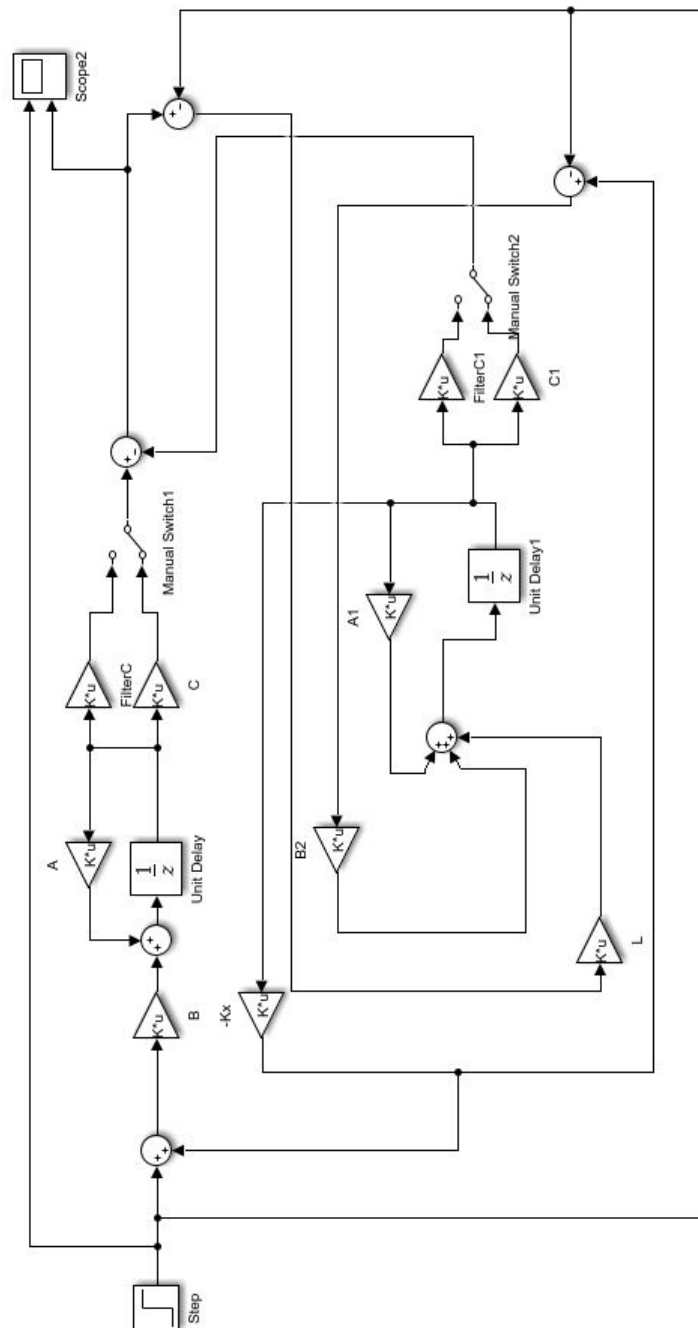
Figure 6.10: State Space scheme with Smith predictor included into the Simulink model

6.6 Conclusion

In this chapter, a review about the state space controller has been performed. The control law and the state estimator have been designed and introduced into the scheme. Then, a modal filter to deal with the high frequency peaks has been described and designed. The Smith predictor has been also presented as a method to deal with the phase lag that appears in the system. This method has been proven to be necessary in order to deal with the instability that appears as an effect of the phase lag. The influence of both methods have not been proven since the state estimator with the Smith predictor could not be implemented into the control scheme. Further research will be needed in this area in order to evaluate the performance of those tools in this system.

Chapter 7

Experiments

In this chapter, the results of the controllers that have been developed in previous chapters is implemented into the machine. First the PID controller is implemented. Then, the additional notch filters are added and also used to control the machine. The effect of the Smith predictor is also measured to the addition and the notch filters. The conclude, the performance of the state space controller has been studied.

7.1 Specifications to meet

To recall from the introduction, several experiments had been presented to show the performance on the controller. In the end, just one experiment has been able to be performed. This experiment is the one with the rotary table. The specifications were limiting the tracking error to 30nm rms in the bandwidth between 0-10 Hz and 4 nm rms between 10-1000Hz. This requirements are with the motor turning at 12rpm.

To reproduce this experiment, a motion controller from the company ETEL has been used, along a software developed by the company called ComET. With this software, it is possible to set the speed to any value desired. The motion controller uses a encoder to measure the position of the rotary table. The aim of using this software is setting the speed to 12 rpm to evaluate the performance of the controller.

Since 3 capacitor sensors are place in the WMF, what is going to be controlled is the average of the measurements of the sensors. They are place approximately 120 deg one from another, so the average of the measurements shows the real position of the centre of the rotary table.
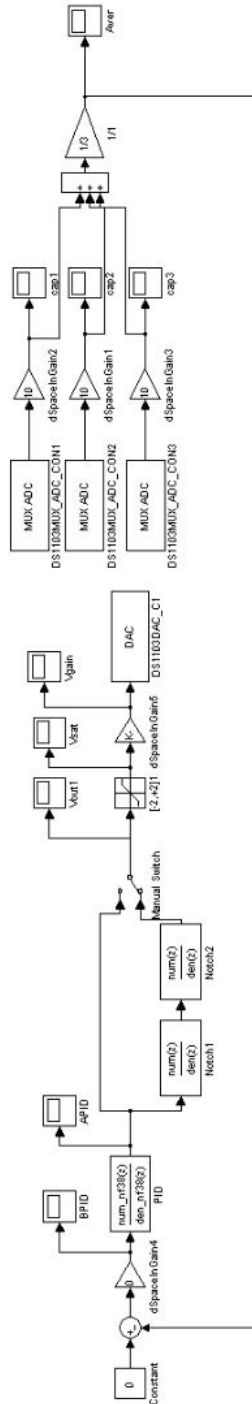
7.2 PID Controller

Figure 7.1: Scheme of the PID controller implemented in Simulink

The first step towards the goal is including the PID controller. In figure 7.1 the Simulink with the Dspace blocks is shown.

Some of the blocks need a further explanation. Gains 1, 2 and 3 are the ones that receive the voltage from Dspace and do it 10 times higher since the values in Dspace are 10 times smaller than in Simulink. Gain 5 does the opposite, by reducing the voltage that Simulink sends to Dspace. Gain 4 is a safety gain. It can be edited in ControlDesk Dspace and its purpose is to prevent the system from start automatically. It just have to be set to either 0 or 1. The DAC and MUX ADC are the blocks that gets in (DAC) and out (MUX ADC) the voltage from Simulink to Dspace. The group of gains 1, 2, 3, 5 and the DAC and MUX ADC blocks, are the plant of the system. Another blocks such as the notch filters, the PID and the gain to do the average can be also seen in the figure. The manual switch can change between using the notch filters or not.

Some controllers designed under the rules of chapter 4 had been implemented into the simulink diagram and tested into the machine. The one with better performance is the one that without the phase lag taken into account reach 161 Hz of bandwidth. The sensibility of the sensors is $2.5\mu m/V$. The graphs are drawn using nm as a unit.
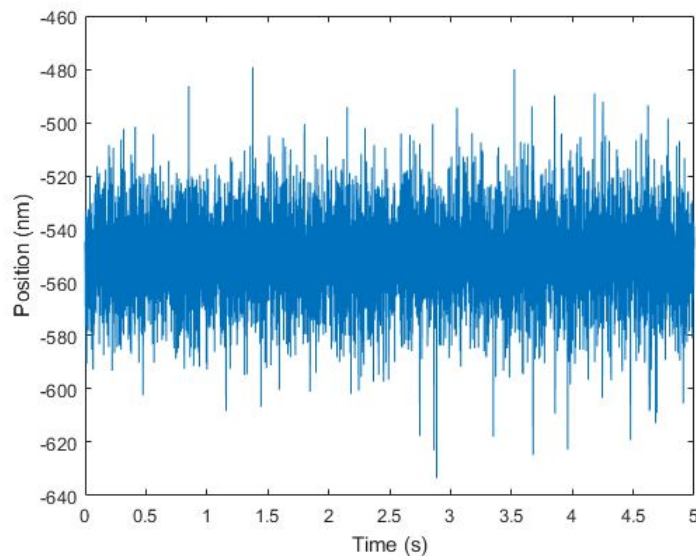

Figure 7.2: Reference set to 0 for the PID controller

The first plot that is shown is the response of the system with the PID just by keeping the average at 0 without any disturbances. Figure 7.2 shows the position

of the workpiece. As it can be seen, the PID cannot follow the reference and the position is not in 0.

The evaluation of how the PID compensates for the disturbances caused by the rotary stage can be seen in figure 7.3. From this graph, it can be seen that the design of the PID cannot follow reference. It shows oscillations that does not match the speed of the rotary table. For instance, a better solution needs to be achieved in order to reach the specifications.
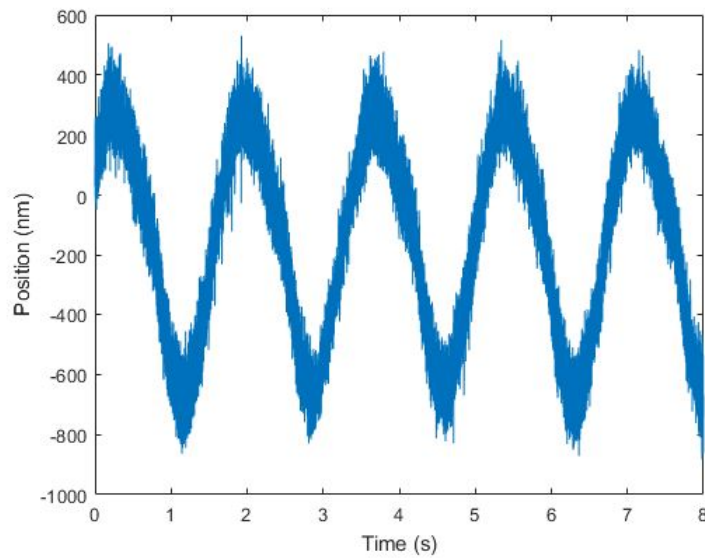
Figure 7.3: Experiment of the rotary table for the PID controller.

7.3 PID and Notch Filters

As the PID is not sufficient, the notch filters has been implemented in order to improve the performance of the controller. To do so, the manual switch in the scheme in figure 7.1 has been activated to used the loop in which the notch filters are included. The bandwidth that is achieved is 290.263 Hz. In figure 7.4 the performance of the controller while just setting the position to 0 nm is displayed.

Comparing with the value from the PID, now with the notch filters included, the result is centred on 0, with a really low disturbance from the initial point. The error for this scheme without disturbances is 5.3437nm rms. It can be observed already that the performance has highly increased with the use of the Notch Filters.

Figure 7.4: Reference set to 0 for the PID controller and the Notch filters.
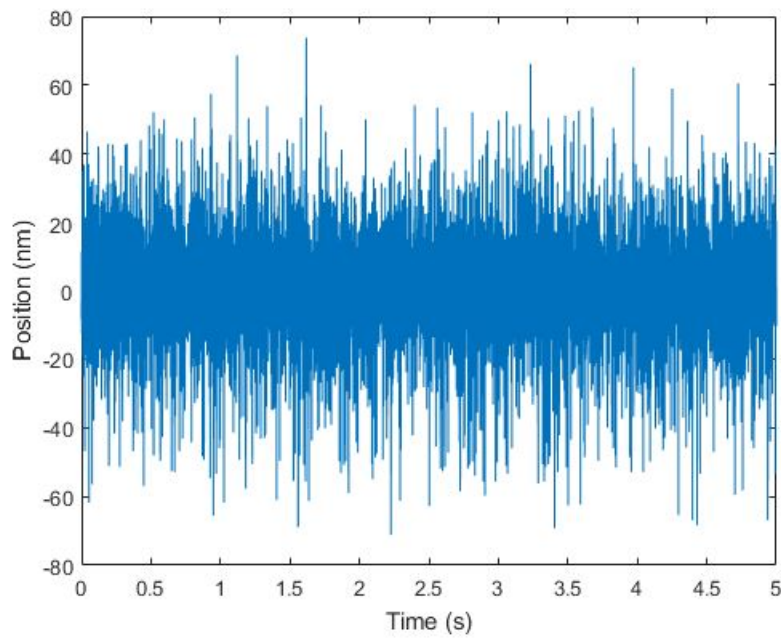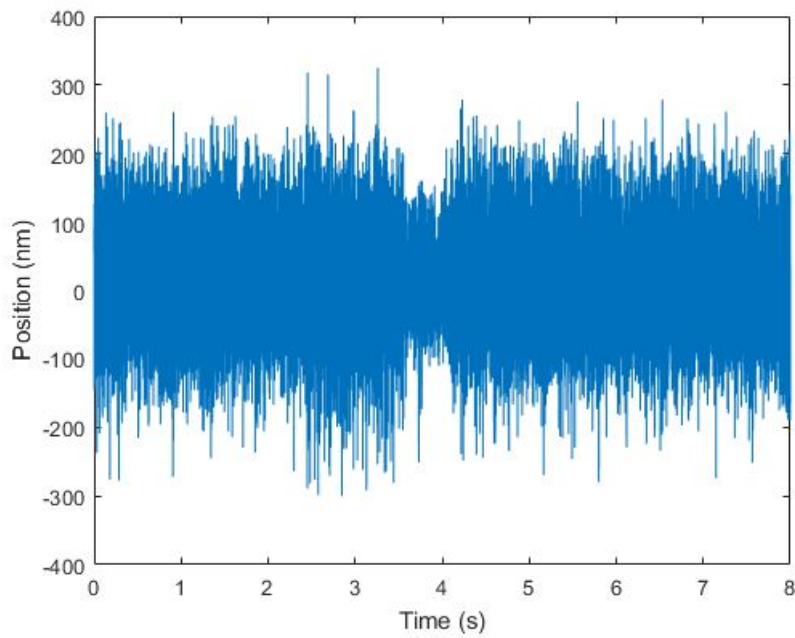

Figure 7.5: Experiment of the rotary table for the PID controller and the notch filters.

57

The experiment of rotating the table is performed, and its results are shown in figure 7.5. An average of 3 measurements has been taken and error goes up to 54.55 nm rms. It does not reach the error under the specifications of the thesis but it is closer than in previous thesis.

7.4 PID, Notch Filters and Smith Predictor

To try to achieve better results, the Smith predictor is implemented into the control scheme. Some modifications have been done in Simulink, in order to include it. The figure 7.7 shows the modifications that has been developed in Simulink.

To the control loop that was designed in 7.1 another loop has been added. The time delay can be seen as well as the plant block. The plant block is the transfer function without delay that was designed in chapter 4. Once the loop is designed, some experiments are performed to check the precision that can be reached. Again the set point of 0 is designed. Figure 7.8 shows the results of the controller keeping the position at 0 without disturbances.

The results of the controller under the effect of the rotary table can be seen in 7.9. An average of 2 results has been perform and an error of 112.77 nm has been obtained. This error is worse than the controller with just the notch filters. This means that adding the Smith predictor decreases the performance of the controller under the same bandwidth
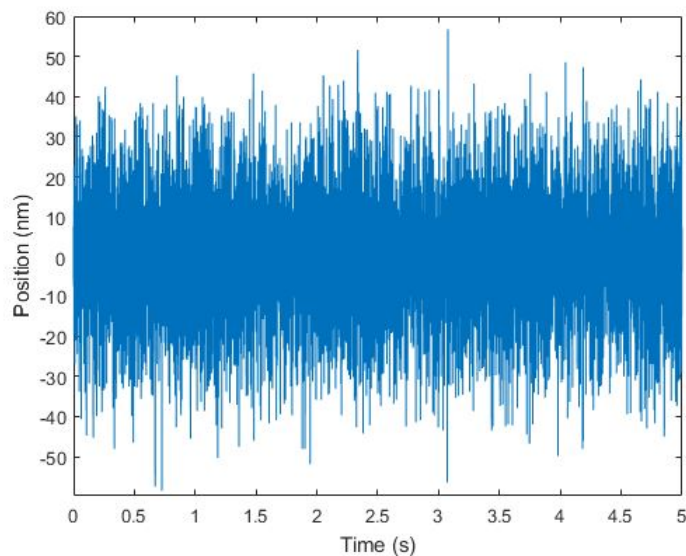
Figure 7.6: Reference set to 0 for the PID controller, the Notch filters and the Smith predictor.
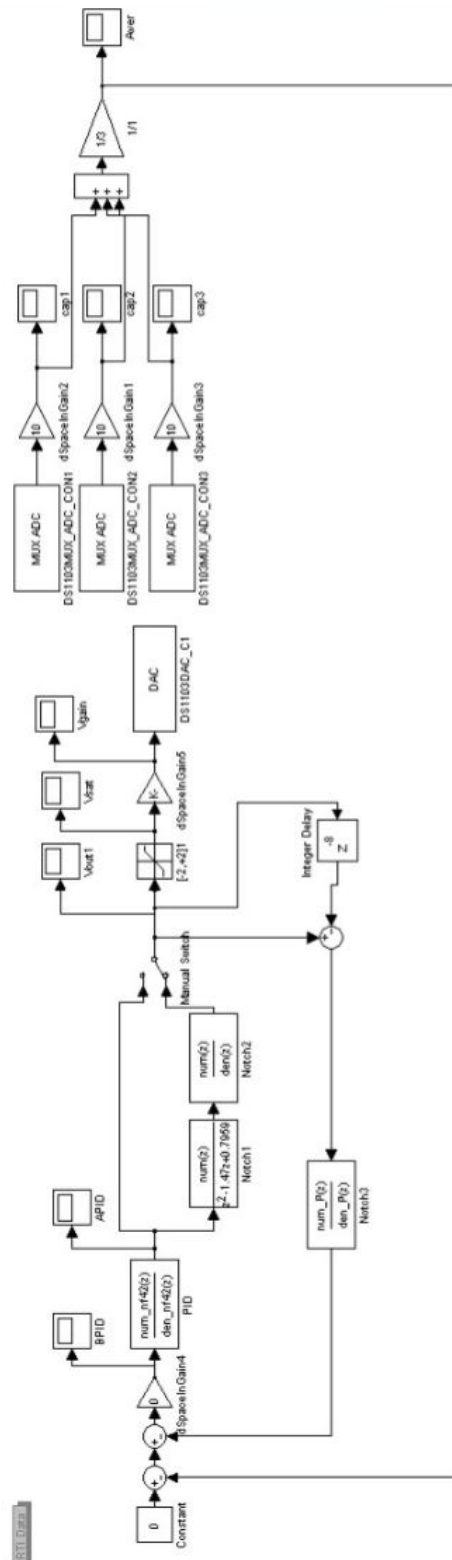
Figure 7.7: Smith Predictor implemented into Dspace blocks in Simulink.
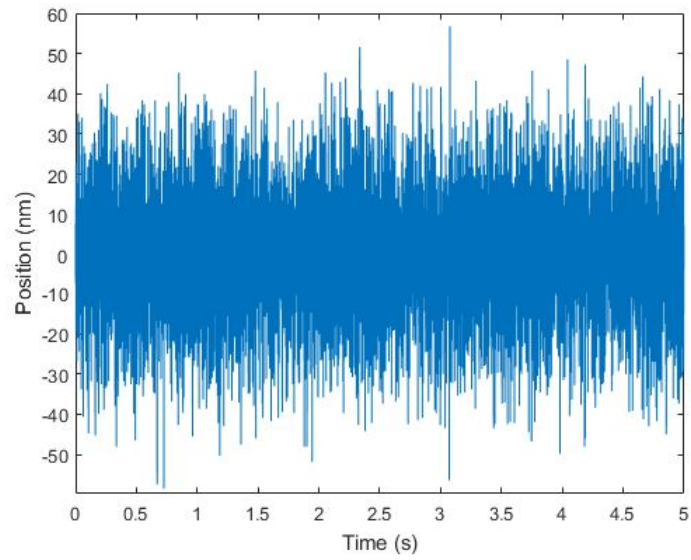
Figure 7.8: Reference set to 0 for the PID controller, the Notch filters and the Smith predictor.
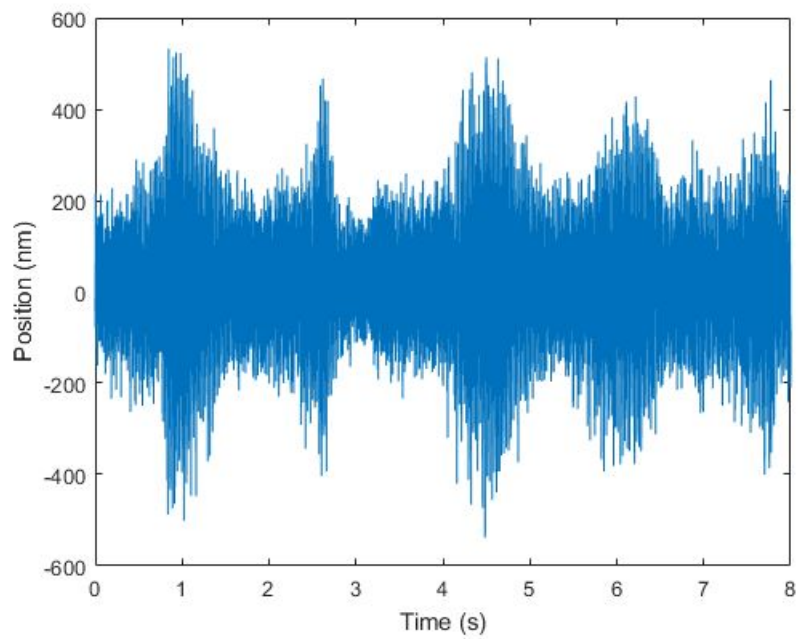
Figure 7.9: Experiment of the rotary table for the PID controller and the Notch filters.

7.4.1 Notch Filter compensation

The lag that has been added to the Smith Predictor is the one calculated in the chapter 4, but notch filters add an extra lag that can also be compensated once the Smith predictor is implemented. For calculating the extra delay, the formula 7.1 is used.

$$\tau = \frac{(\phi_r - \phi_e)}{360 \cdot 1000} = 8.33 \cdot 10^{-5} s \tag{7.1}$$

This is equivalent of a delay of four time steps. This delay added to the eight time steps that it was due to the delay compensation sums up until around twelve time steps. Some experiments are perform to see if this variation affects to the final control.
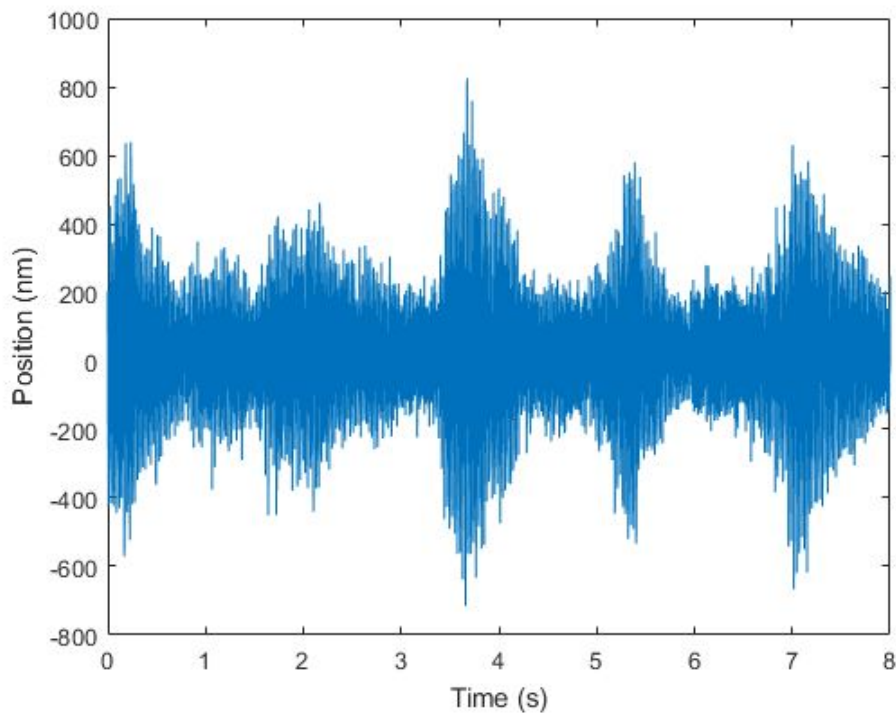
Figure 7.10: Experiment of the rotary table for the PID controller and the Notch filters.

Figure 7.10 shows the performance with the lag of the notch filters added to the lag that it was within the system. The performance drops and so does the error that reaches 161.066nm keeping the same bandwidth. Besides this results, it is also important to remark that a higher bandwidth have been tried with the Smith

predictor. In the case when the delay was set to 8, the system was unstable, but when a higher time delay was added due to the notch filters, the system became more stable, even thought the results were far from good. This means that with the use of the Smith Predictor, the system became more stable but the performance decrease. Results with a bandwidth of Hz are shown in figure 7.11.
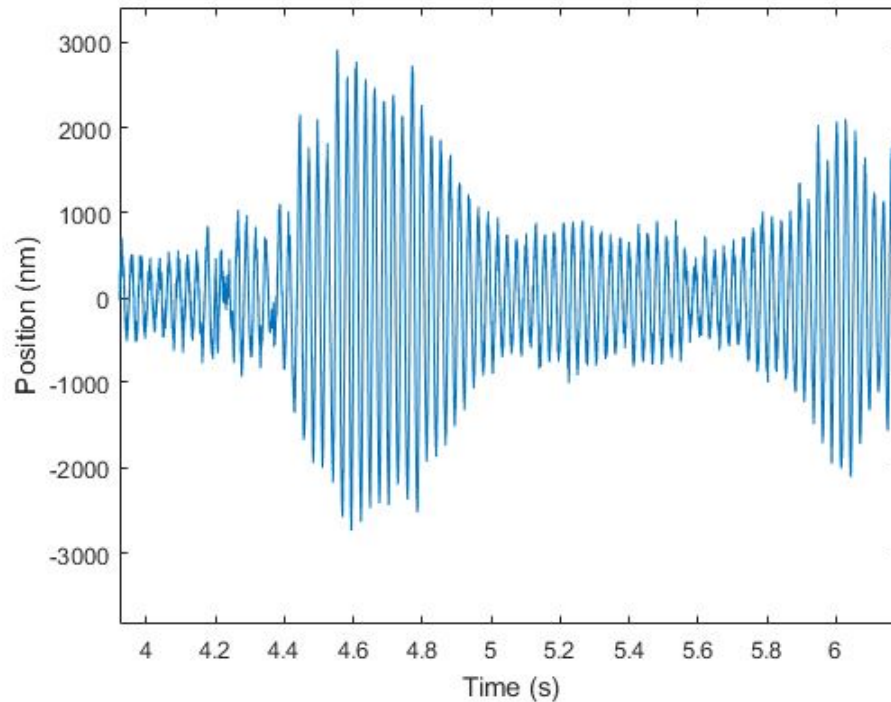
Figure 7.11: Experiment of the rotary table for the PID controller and the Notch filters.

7.5 State Space Validation

An scheme of the state space controller has been implemented into Simulink. The plant looks as in figure 7.12. Some of the blocks that appear in the PID controller also appear in the state space scheme, specially the ones related to the Dspace blocks. It can also be seen the modal filter implemented. It corresponds to the C matrix. The switch allows to change between the C matrix and the C matrix filtered. The experiment has been performed ans a result reflected in 7.13 is obtained. The error, nevertheless, is higher than in any case of the PID controller, so further research have to be done in this type of controller in order to compete with PID characteristics.
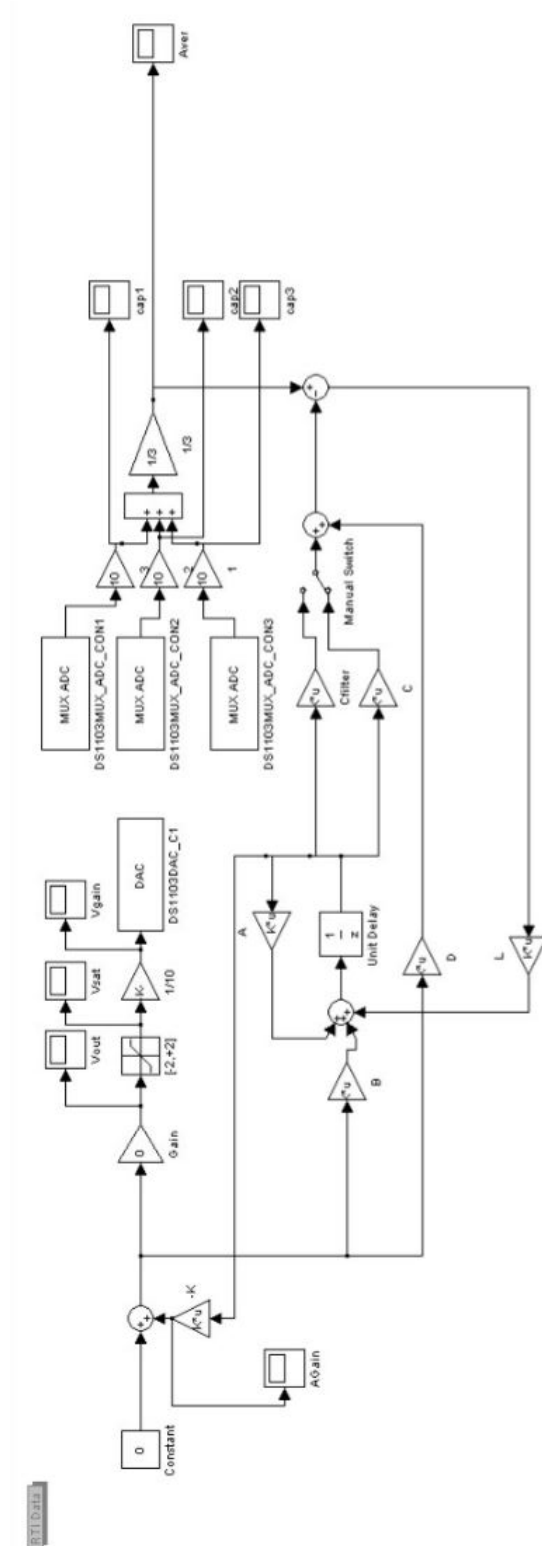
Figure 7.12: Scheme of the state space implemented in the Dspace Simulink
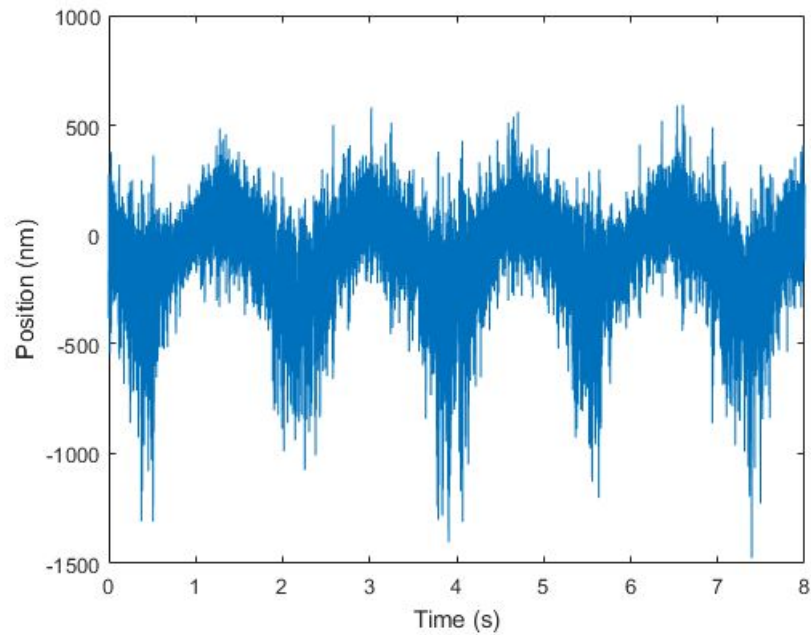
Figure 7.13: Experiment of the rotary table for the state space controller

7.6   Conclusion

In this chapter, the different ways that have been developed during the Thesis have been implemented into the machine. As a result, the configuration with the PID and the notch filters is the one that gets lesser error, with 56nm rms. The addition of the Smith predictor did not improve the control but it improved the stability when reaching higher bandwidth. As expected, the results of the state space controller, were not better as the ones from the PID due to the lag compensation could not be added.

Chapter 8

Conclusion

To obtain an accurate positioning, a good control design is essential. The scope of this thesis has been the design of the controller to achieve the precision needed for the grinding machine. The controller has to be applied in the VCA (voice coil actuator) to prevent the disturbances of the process to modify the position of the workpiece. Some control strategies have been studied in the literature review.

The first step has consisted to do a correct identification of the system. For this purpose the VCA has been excited with a multisine signal to obtain the transfer function that represents the system. This identification has been done several times since problems with the current source have appeared during the development of the thesis. The identified transfer function has also been matched with a model that has been performed into MATLAB Simulink with the physical properties of the system. The aim of the model is to identify what is the cause of the frequency peaks.

While identifying the system some problems have been encountered. The first one is a time delay in the system that is caused by the acquisition data system. This problem might affect the control in a way that less phase margin can be obtained. The other problem is a bandwidth limiting frequency peaks that can make the control to cross the 0 dB line twice.

Two different approaches have been taken to design the controller. The first control scheme that has been studied is a PID Controller. The PID has been designed by a procedure explained in [18] . Another design has been made and a state space controller has been designed also by following the guidelines from [18].

In order to deal with the problems encountered, different methods have been implemented in both controllers. In the PID scheme, two notch filters have been created to prevent the high frequency peaks to disturb the control action. Also, a Smith predictor has been applied to deal with the time delay. In the case of the state space system, a modal filtering is used. This filter is created to cancel the poles that creates the high frequency peaks. To compensate the time delay, an attempt of the Smith predictor has

65

been tried in the state space scheme but the correct configuration has not been found.

Several experiments have been performed into the machine by turning the rotary table with a constant speed and checking how much the deviation from the desired position was. The configuration that got better results is a PID that reached 260Hz of bandwidth with both notch filters implemented. The error obtained is 56nm rms. The Smith predictor has been proved to not improve the accuracy but it can turn the system more stable with higher bandwidth.

Future work

Not all the experiments that have been proposed could have been performed so the first step would be to complete the other experiments to see if the control in those cases is good enough. Otherwise, knowing how far the control designed is from the specifications would be the first step to set a new goal.

Regarding the design of the control, a way to include the Smith predictor into the state space scheme with an estimator might be key to get higher in frequency, due to the fact that the modal filtering is more reliable than the notch filters since it flatten more the signal.

To handle the delay, the Smith predictor has been proven to be not sufficient when the objective is getting more disturbance rejection. For this reason,it is suggested to look for another way of structuring the Smith predictor into the PID scheme.

Appendices

Appendix A

Model Parameters

Parameter	Value	Units
m_{shaft}	5.7	kg
$m_{\text{z-base}}$	66	kg
m_{WMF}	38	kg
m_{cmass}	11.1	kg
k_{cmass}	1.66	$N/\mu m$
c_{cmass}	85.9	$N/ms^{\text{-1}}$
k_{flex}	0.332	$N/\mu m$
c_{flex}	27.5	$N/ms^{\text{-1}}$
k_{fix}	29	$N/\mu m$
c_{fix}	2100	$N/ms^{\text{-1}}$
k_{table}	0.166	$N/\mu m$
c_{table}	100	$N/ms^{\text{-1}}$
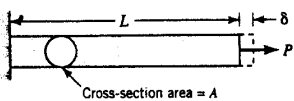
Table A.1: Mass, damping and stiffness values of the Simulink model.

Appendix B

Files needed for the calculation of the stiffness

TABLE 5.1 Deflection and Stiffness Formulas for Straight Bars (Rods, Beams) of Uniform Section

Number	Case	Deflection	Spring Rate
1.	Tension or compression Cross-section area $= A$	$\delta = \dfrac{PL}{AE}$	$k = \dfrac{P}{\delta} = \dfrac{AE}{L}$
2.	Torsion K'^a = section property. For solid round section, $K' = J = \pi d^4/32$.	$\theta = \dfrac{TL}{K'G}$ For solid round bar and deflection in degrees, $\theta^o = \dfrac{584TL}{d^4 G}$	$K = \dfrac{T}{\theta} = \dfrac{K'G}{L}$
3.	Bending (angular deflection) I = moment of inertia about neutral bending axis	$\theta = \dfrac{ML}{EI}$	$K = \dfrac{M}{\theta} = \dfrac{EI}{L}$
4.	Bending (linear deflection) I = moment of inertia about neutral bending axis	$\delta = \dfrac{ML^2}{2EI}$	$k = \dfrac{M}{\delta} = \dfrac{2EI}{L^2}$
5.	Cantilever beam loaded at end I = moment of inertia about neutral bending axis	$\delta = \dfrac{PL^3}{3EI}$	$k = \dfrac{P}{\delta} = \dfrac{3EI}{L^3}$

Note: See Appendixes A-4 and A-5 for appropriate SI units and prefixes.
[a]See Table 5.2 for values of K' for other sections.
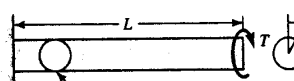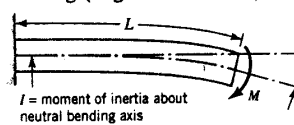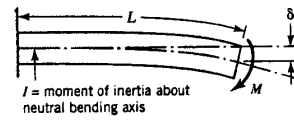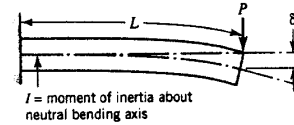
TABLE 5.3 Summary of Energy and Deflection Equations for Use with Castigliano's Method

Load Type (1)	Factors Involved (2)	Energy Equation for Special Case Where All Three Factors Are Constant with x (3)	General Energy Equation (4)	General Deflection Equation (5)
Axial	P, E, A	$U = \dfrac{P^2 L}{2EA}$	$U = \int_0^L \dfrac{P^2}{2EA}\,dx$	$\Delta = \int_0^L \dfrac{P(\partial P/\partial Q)}{EA}\,dx$
Bending	M, E, I	$U = \dfrac{M^2 L}{2EI}$	$U = \int_0^L \dfrac{M^2}{2EI}\,dx$	$\Delta = \int_0^L \dfrac{M(\partial M/\partial Q)}{EI}\,dx$
Torsion	T, G, K'	$U = \dfrac{T^2 L}{2GK'}$	$U = \int_0^L \dfrac{T^2}{2GK'}\,dx$	$\Delta = \int_0^L \dfrac{T(\partial T/\partial Q)}{GK'}\,dx$
Transverse shear (rectangular section)	V, G, A	$U = \dfrac{3V^2 L}{5GA}$	$U = \int_0^L \dfrac{3V^2}{5GA}\,dx$	$\Delta^a = \int_0^L \dfrac{6V(\partial V/\partial Q)}{5GA}\,dx$

[a]Change constant $\tfrac{6}{5}$ to 1 for quick *estimates* involving nonrectangular sections [3].

Figure B.1: Transfer function of a Notch filter
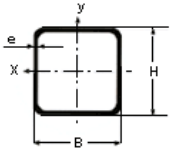
Tubos estructurales cuadrados

Dimensiones		Peso p (kg/m)	Sección A (cm²)	EJE X				Inercia a la torsión IT (cm4)
H X B (mm)	e (mm)			Momento de Inercia Ix (cm⁴)	Módulo resistente Wx (cm³)	Módulo de plasticidad Sx (cm³)	Radio de giro ix (cm)	
50 x 50	2,5	3,54	4,51	17,9	7,16	8,47	1,99	26,8
	3,0	4,22	5,37	20,8	8,34	9,95	1,97	31,1
	4,0	5,52	7,03	26,2	10,46	12,73	1,93	38,9
	5,0	6,78	8,64	30,8	12,30	15,25	1,89	45,6
60 x 60	2,0	3,60	4,58	26,0	8,68	10,10	2,38	39,0
	3,0	5,32	6,78	37,1	12,38	14,63	2,34	55,6
	4,0	7,00	8,92	47,1	15,69	18,85	2,30	70,2
	5,0	8,63	10,99	55,9	18,64	22,75	2,26	83,2
70 x 70	2,0	4,34	5,53	42,0	11,99	13,88	2,76	62,9
	3,0	6,43	8,20	60,3	17,22	20,21	2,71	90,2
	4,0	8,48	10,80	76,9	21,98	26,17	2,67	115,0
	5,0	10,48	13,35	92,1	26,31	31,75	2,63	137,3
75 x 75	2,0	4,54	5,78	51,9	13,84	15,99	3,00	77,8
	3,0	6,73	8,57	74,8	19,94	23,34	2,95	112,0
	4,0	8,87	11,30	95,7	25,53	30,28	2,91	143,2
	5,0	10,97	13,97	114,9	30,64	36,81	2,87	171,5
80 x 80	2,0	4,83	6,15	63,3	15,83	18,26	3,21	94,9
	3,0	7,17	9,14	91,4	22,86	26,69	3,16	137,0
	4,0	9,47	12,06	117,4	29,35	34,69	3,12	175,6
	5,0	11,71	14,92	141,3	35,31	42,25	3,08	210,9
	6,0	13,90	17,71	163,2	40,79	49,39	3,04	243,1

Figure B.2: Inertia squared structural tubes

Bibliography

[1] K. H. Ang, G. Chong, and Y. Li. Pid control system analysis, design, and technology. *IEEE transactions on control systems technology*, 13(4):559–576, 2005.

[2] T. G. ans J. Eisinger, R. ans D. Laroans J. van Eijk, and M.Steinbuch. Direction based filtering of flexible modes. In *American Society for Precision Engineering Conference, 2013. Proceedings of the 2013*, volume 56, pages 32–38. ASPE, 2013.

[3] K. J. Åström and T. Hägglund. Revisiting the ziegler–nichols step response method for pid control. *Journal of process control*, 14(6):635–650, 2004.

[4] Y. Cao. Correcting the minimum itae standard forms of zero-displaceemnt-error systems. *Journal of Zhejiang University (Natural Science)*, 23(4):550–559, 1989.

[5] S.-B. Choi, W. Li, M. Yu, H. Du, J. Fu, and P. X. Do. State of the art of control schemes for smart systems featuring magneto-rheological materials. *Smart Materials and Structures*, 25(4):043001, 2016.

[6] M. Dahleh, A. Munther, G. Dahleh, and Verghese. *Lectures on Dynamic Systems and Control.* Department of Electrical Engineering and Computer Science, MIT, 2011.

[7] W. East and B. Lantz. *Notch filter Design.* August 29, 2005.

[8] F. Fang, X. Zhang, A. Weckenmann, G. Zhang, and C. Evans. Manufacturing and measurement of freeform optics. *CIRP Annals-Manufacturing Technology*, 62(2):823–846, 2013.

[9] D. Hemschoote. *Ultra Precision Five-Axis ELID Grinding Machine: Design and Prototype Development.* Belgium: KU Leuven, University of Leuven, 2008.

[10] D. Houben. *Design and validation of a workpiece metrology frame for an ultra-precision five-axis grinding machine.* Belgium: KU Leuven, University of Leuven, 2016.

[11] R. Jehoul. *Controle en experimentele validatie van een rotatief-lineaire actuator voor een nanometernauwkeurige vijfassige slijpmachine.* Belgium: KU Leuven, University of Leuven, 2016.

[12] K. Kim, Y. Kim, L. Keel, and S. Bhattacharyya. Pid controller design with time response specifications. In *American Control Conference, 2003. Proceedings of the 2003*, volume 6, pages 5005–5010. IEEE, 2003.

[13] M. Lubini, M. Sereno, J. Coles, P. Jetzer, and P. Saha. Cosmological parameter determination in free-form strong gravitational lens modelling. *Monthly Notices of the Royal Astronomical Society*, 437(3):2461–2470, 2013.

[14] M. A. Moiseev, L. L. Doskolovich, and N. L. Kazanskiy. Design of high-efficient freeform led lens for illumination of elongated rectangular regions. *Optics express*, 19(103):A225–A233, 2011.

[15] S. Mori, M. Furuya, A. Naganawa, Y. Shibuya, G. Obinata, and K. Ouchi. Nano-motion actuator with large working distance for precise track following. *Microsystem technologies*, 13(8-10):873–881, 2007.

[16] D. Neyens and Z. Van Campen. *Design of a combined rotary linear actuator for a nanometer precision five-axis grinding machine*. Belgium: KU Leuven, University of Leuven, 2015.

[17] A. O'Dwyer and J. Ringwood. A classification of techniques for the compensation of time delayed processes. part 2: Structurally optimised controllers. *Arrow@DIT*, 1999.

[18] G. Pipeleers and J. Swevers. *Control Theory*. Belgium: KU Leuven, University of Leuven, 2016.

[19] J. Speyer. Computation and transmission requirements for a decentralized linear-quadratic-gaussian control problem. *IEEE Transactions on Automatic Control*, 24(2):266–269, 1979.

[20] J. Swevers. *Slides from Advanced Model Based Control*. Belgium: KU Leuven, University of Leuven, 2008.

[21] D. Warwick and D. Rees. *Industrial Design Control Systems*. IET, 1988.

Master's thesis filing card

Student: Pablo Carbonell Romero

Title: Control design of a short-stroke workpiece actuator for error motion compensation

UDC: 621

Abstract:

The prototype of a five axis ELID grinding machine is being developed at KU Leuven. The scope of this machine is the production of lenses with nanometer accuracy. For obtaining this level of precision a robust controller has to be designed to minimize the disturbances of the process. In previous theses a VCA (voice coil actuator) was studied an implemented. The aim of this project is to design a controller that uses the VCA to reject the disturbances created by the grinding forces as well as other disturbances. transfer function of the system has to be identified through excitation of the machine. Once the transfer function is obtained, the controller needs to be implemented. The first controller designed is a PID controller. A state space based controller has also been designed, but due to a problem with time delay it has not been implemented into the setup. While developing the controller, two problems have been encountered: time delay and bandwidth limiting resonance peaks. To solve time delay, a control structure called Smith predictor has been implemented into the machine. To compensate the bandwitdth limiting peaks, Notch filters have been designed and introduced into the control scheme. With the controllers that have been designed, the last step is to see how the grinding machine performs under the effect of the disturbance produced by the rotary table. The table rotates at a speed of 12rpm. By adding the notch filters and the Smith predictor, an error of 56nm rms is obtained under a frequency of 260Hz.

Thesis submitted for the degree of Master of Science in Mechanical Engineering

Thesis supervisor: Prof. dr. ir. Dominiek Reynaerts

Assessors: Dr. ir. Goele Pipeleers
           Dr. Jun Qian

Mentor: Dr. ir. Niels Bosmans